Molecular characteristics and diurnal variations of organic aerosols at a rural site in the North China Plain with implications for the influence of regional biomass burning

Jianjun Li[1,4], Gehui Wang[1,2,3] *, Qi Zhang[4*], Jin Li[1], Can Wu[2], Wenqing Jiang[4], Tong Zhu[5], and Limin Zeng[5]

[1]Key Lab of Aerosol Chemistry & Physics, SKLLQG, Institute of Earth Environment, Chinese Academy of Sciences, Xi'an 710061, China
[2]Key Laboratory of Geographic Information Science of the Ministry of Education, School of Geographic Sciences, East China Normal University, Shanghai 200241, China
[3]Institute of Eco-Chongming, 3663 N. Zhongshan Rd., Shanghai 200062, China
[4]Department of Environmental Toxicology, University of California, Davis, CA 95616, USA
[5]BIC-ESAT and SKL-ESPC, College of Environmental Sciences and Engineering, Peking University, Beijing, China

*Corresponding authors:
Prof. Gehui Wang, E-mail: ghwang@geo.ecnu.edu.cn;
Prof. Qi Zhang, E-mail: dkwzhang@ucdavis.edu

Abstract

Field burning of crop residue in early summer releases into the atmosphere a large amount of pollutants with significant impacts on the air quality and aerosol properties in the North China Plain (NCP). In order to investigate the influence of this regional anthropogenic activity on molecular characteristics of organic aerosols, $PM_{2.5}$ filter samples were collected with a 3-hr interval at a rural site of NCP from June 10th to 25th, 2013, and analyzed for more than 100 organic tracer compounds, including both primary (*n*-alkanes, fatty acids/alcohols, sugar compounds, polycyclic aromatic hydrocarbons, hopanes, and phthalate esters) and secondary organic aerosol (SOA) tracers (phthalic acids, isoprene-, α-/β-pinene, β-caryophyllene, and toluene-derived products), as well as organic carbon (OC), elemental carbon (EC), and water-soluble organic carbon (WSOC). Total concentrations of the measured organics ranged from 177 to 6248 ng m^{-3} (mean 1806 ± 1308 ng m^{-3}) during the study period, most of which were contributed by sugar compounds, followed by fatty acids and fatty alcohols. Levoglucosan (240 ± 288 ng m^{-3}) was the most abundant single compound and strongly correlated with OC and WSOC, suggesting that biomass burning (BB) is an important source of summertime organic aerosols in this rural region. Based on the analysis of fire spots and backward trajectories of air masses, two representative periods were classified, which are (1) Period 1 (P1), Jun 13th 21:00-16th 15:00, when air masses were uniformly from the southeast part of NCP, where intensive open-field biomass burning occurred; and (2) Period 2 (P2), Jun 22nd 12:00-24th 06:00, which is representative of local emission. Nearly all the measured PM components showed much higher concentrations in P1 than in P2. Although *n*-alkanes, fatty acids, and

fatty alcohols presented similar temporal/diurnal variations as those of levoglucosan

throughout the entire period, their molecular distributions were more dominated by

high molecular weight (HMW) compounds in P1, demonstrating an enhanced

contribution from BB emissions. In contrast, intensive BB emission in P1 seems to

have limited influences on the concentrations of polycyclic aromatic hydrocarbons

(PAHs), hopanes and phthalate esters. Both 3-hydroxyglutaric acid and β-

caryophyllinic acid showed strong linearly correlations with levoglucosan (R^2=0.72

and 0.80, respectively), indicating that BB is also an important source for terpene-

derived SOA formation. A tracer-based method was used to estimate the distributions

of biomass-burning OC, fungal-spore OC and secondary organic carbon (SOC)

derived from isoprene, α-/β-pinene, β-caryophyllene, and toluene in the different

periods. The results showed that the contribution of biomass-burning OC to total OC

in P1 (27.6%) was 1.7 times of that in P2 (17.1%). However, the contribution of SOC

from oxidation of the four kinds of volatile organic compounds (VOCs) increased

slightly from 16.3% in P1 to 21.1% in P2.

Key words: Organic aerosols; Molecular composition; North China Plain; Biomass

Burning

1. Introduction

Organic aerosols (OA, i.e., the organic fraction of particles) constitute a substantial fraction (~10-90%) of atmospheric particles (Jimenez et al., 2009;Zhang et al., 2007a;Hallquist et al., 2009), and have significant effects on global and regional climate (Venkataraman et al., 2005;Kanakidou et al., 2005), air quality (Aggarwal et al., 2013;Wang et al., 2006b), human health (Lelieveld et al., 2015), and ecosystems (Tie et al., 2016). Organic aerosols in the atmosphere can be emitted directly from various sources, such as fossil fuels combustion, biomass burning, plant emission, and so on, which is defined as primary organic aerosols (POA). On the other hand, atmospheric secondary OA (SOA) are produced from photochemical oxidation products of volatile organic compounds (VOCs) via gas-particle conversion processes such as nucleation, condensation and heterogeneous chemical reactions (Hallquist et al., 2009). These organic species could modify physicochemical characteristics of atmospheric aerosols such as hygroscopicity, albedo, and oxidation state (Dinar et al., 2008;Chan et al., 2005;Fu et al., 2010). Thus, a thorough understanding of molecular composition and source of organic aerosols is necessary in order to address aerosol related environmental issues and to improve the accuracy of modelling studies.

Tremendous amounts of air pollutants including both particulate matters (PM) and their gaseous precursors (e.g., SO_2, NO_x, NH_3, and VOCs) are emitted into the atmosphere from power plants, industries and vehicles due to rapid economy development in China, leading to serious air pollution in the recent decades (Zhang et al., 2009;Guo et al., 2014;Wang et al., 2016;Huang et al., 2014;Li et al., 2017). The

92 North China Plain (NCP) has been recognized as one of the most polluted regions in

93 the world, with very high concentrations of $PM_{2.5}$ on the ground surface (van Donkelaar

94 et al., 2010). The NCP is also one of the most significant aerosol sources in the world,

95 which has a significant impact on the East China Sea and Western North Pacific

96 (Andreae and Rosenfeld, 2008). Thus, extensive efforts have been made in recent years

97 to characterize the sources, properties, and processes of PM in the NCP. Most of these

98 results concluded that the severe air pollution in the region is related to the source

99 strength and frequently happens under stagnant weather conditions. Recent studies

100 showed that the rapid growth of secondary aerosols could lead to an severe haze event

101 in China under certain meteorological conditions (Wang et al., 2016;Sun et al.,

102 2014;Quan et al., 2013).

103   In the rural area of NCP, biomass burning for domestic cooking and heating, and

104 agricultural waste disposal is an important source of atmospheric PM (Wang et al.,

105 2009b;Li et al., 2010;Zhang et al., 2016). Particularly, the open-field burning is still a

106 common way for disposal of crop residues (mainly wheat straw) in early summer (Li

107 et al., 2007). This traditional activity could release huge amounts of pollutants into the

108 atmosphere and significantly affect air quality and aerosol properties in the region.

109 Zhu et al. (2016) examined the amounts of VOCs in the air at a rural site of Yucheng

110 (Shandong Province, East China), and found that their concentrations during the

111 wheat straw burning period are approximately twice of those in normal periods.

112 Model results also revealed a significant influence of open crop residual burning on

113 ozone, CO, black carbon (BC) and organic carbon (OC) concentrations in NCP.

114 Moreover, both off-line (Fu et al., 2012;Wang et al., 2009b;Wang et al., 2011) and

115 on-line (Sun et al., 2016) observations indicated that the intensive emission from

116 wheat straw burning in the region could change the molecular distribution of organic

117 aerosols in the downwind urban or mountain areas.

118   During June 10th to 25th of 2013, we conducted a continuous sampling campaign

119 at a rural site in the northern part of NCP. PM$_{2.5}$ filter samples were collected with a

120 3-hour time resolution and determined for more than 100 organic compounds

121 including aliphatic lipids, sugar compounds, hopanes, polycyclic aromatic

122 hydrocarbons (PAHs), phthalate esters, and secondary oxidation products. The first

123 objective of this study was to get an overall understanding of temporal/diurnal

124 variation and molecular distribution of summertime OA in the rural region. The

125 second objective was to compare the results in two representative periods to

126 investigate the influence of regional field burning of wheat straw on the molecular

127 characteristics of organic aerosols.

128 **2. Experimental section**

129 **2.1 Sample collection**

130   The sampling was performed at the Integrated Ecological-Meteorological

131 Observation and Experiment Station of Chinese Academy of Meteorological Sciences

132 (39°08' N, 115°40' E, 15.2 m a.s.l.), which is located in a rural area of Gucheng,

133 Hebei Province. Detailed information of the station and sampling campaign was

134 described in Li et al. (2018). Briefly, time-resolved (06:00–09:00, 09:00–12:00,

135 12:00–15:00, 15:00–18:00, 18:00–21:00, 21:00–24:00, 00:00–03:00, and 03:00–

06:00, Beijing time) PM$_{2.5}$ samples were collected on the rooftop (about 10 m above

the ground) of a three-story building on the campus of the Gucheng station. The

sampling was conducted by using a high volume (1.13 m^3 min^{-1}) sampler (Anderson)

with a PM$_{2.5}$ inlet from June 10th to 25th, 2013. This period was chosen, because open-

field burning of wheat straw in NCP mainly occur in the mid of June. All samples

were collected onto pre-baked (450 ^{o}C, 6-8 hr) quartz fiber filters. Field blank samples

were also collected by mounting blank filters onto the sampler for about 15 min

without pumping any air. After sampling, the sample filter was individually sealed in

aluminum foil bags and stored in a freezer (−20 ^{o}C) prior to analysis.

2.2 Organic compounds determination

A size of 12.5-25 cm^2 of the filter sample was cut and extracted with a mixture of

dichloromethane and methanol (2:1, v/v) under ultrasonication. The extracts were

concentrated using a rotary evaporator under vacuum conditions and then blow down

to dryness using pure nitrogen. After reaction with N,O-bis-(trimethylsilyl)

trifluoroacetamide (BSTFA) at 70 ℃ for 3 hrs., the derivatives were determined

using gas chromatography/electron ionization mass spectrometry (GC/EI-MS) (Li et

al., 2013b).

GC/EI-MS analysis of the derivatized fraction was performed using an Agilent

7890A GC coupled with an Agilent 5975C MSD. The GC separation was carried out

on a DB-5MS fused silica capillary column with the GC oven temperature

programmed from 50℃ (2 min) to 120℃ at 15℃ min^{-1} and then to 300℃ at 5℃

min^{-1} with a final isothermal hold at 300℃ for 16 min. The sample was injected in a

158   splitless mode at an injector temperature of 280℃, and scanned from 50 to 650

159   Daltons using electron impact (EI) mode at 70 eV.

160   GC/EI-MS response factors of all the target compounds were determined using

161   authentic standards except several isoprene-derived SOA tracers. Response factors of

162   isoprene-derived SOA tracers were substituted by those of related surrogated

163   standards, which were described in Li et al. (2018). No significant contamination

164   (<5% of those in the samples) was found in the blanks. Recoveries of all the target

165   compounds ranged from 80% to 120%. Data presented were corrected for the field

166   blanks but not corrected for the recoveries.

167   **2.3 OC, EC, and WSOC analysis**

168   OC (organic carbon) and EC (elemental carbon) were analyzed using DRI Model

169   2001 Carbon Analyzer following the Interagency Monitoring of Protected Visual

170   Environments (IMPROVE) thermal/optical reflectance (TOR) protocol. A size of

171   0.526 cm^2 sample filter was placed in a quartz boat inside the analyzer and stepwise

172   heated to temperatures of 140 ℃ (OC1), 280 ℃ (OC2), 480 ℃ (OC3), and

173   580 ℃ (OC4) in non-oxidizing helium (He) atmosphere, and 580 ℃ (EC1), 740 ℃

174   (EC2), and 840 ℃ (EC3) in an oxidizing atmosphere of 2% oxygen in helium.

175   Pyrolyzed carbon (PC) is determined by reflectance and transmittance of 633 nm

176   light. One sample was randomly selected from every 10 samples and re-analyzed.

177   Differences determined from the replicate analyses were <5% for TC, and <10% for

178   OC and EC.

179   Another aliquot of filter sample was extracted with organic-free Milli-Q water

180   under ultrasonication (15 min each, repeated 3 times) and filtered through a PTFE

181   filter to remove any particles and filter debris. Then the water-extract was analyzed

182   for water-soluble organic carbon (WSOC) using a TOC analyzer (TOC-L CPH,

183   Shimadzu, Japan). The difference between OC and WSOC was considered as water-

184   insoluble OC (WIOC). All carbonaceous components data reported here were

185   corrected by the field blanks.

186   **3. Results and discussion**

187   **3.1 Fire spots and air masses**

188   At present, open-field burning is still a common activity for disposal of crop

189   residue in the rural area of the North China Plain, especially during wheat harvest period

190   from the end of May to the middle of June (Fu et al., 2012). These extensive emissions

191   from regional biomass burning in the provinces of Anhui, Jiangsu, Shandong, Henan

192   and Hebei in NCP can cause severe air pollution on a local and regional scale. In our

193   previous study, the fire spots in NCP during the sampling period were provided based

194   on the NASA satellite observation (https://firms.modaps.eosdis.nasa.gov/firemap/).

195   Combining   with   information   on   air   mass   back-trajectories

196   (http://ready.arl.noaa.gov/HYSPLIT.php), the sampling period was divided into two

197   sections: (1) June 10-18, when air masses were mainly transported via long distances

198   from the southeast part of NCP, where intensive emissions from wheat straw burning

199   occurred; (2) June 19-25, when air masses were mostly influenced by local emissions

200   and regional emission from biomass burning decreased dramatically (Li et al., 2018).

201   In this study, we further selected two representative periods to estimate the contribution

202 of regional biomass burning. Period 1 (P1) designates 13th Jun 21:00 pm to 16th Jun

203 15:00 pm, during which air masses were influenced by intensive biomass burning and

204 transported uniformly from the southeast part of NCP (Figure 1 a and b, and Figure S1).

205 Period 2 (P2) designates 22nd Jun 12:00 pm to 24th Jun 06:00 am, during which fire

206 spots in the regions were relatively scarce and air masses came predominantly from the

207 surrounding areas of the sampling site (Figure 1 c and d). In addition, there were several

208 intermittent rainfalls during June 20th -22nd, which are favorable for wet deposition of

209 atmospheric pollutants. Thus, aerosols collected in P2 are well representative of local

210 fresh emission. It is worthwhile to note that the two samples collected during 21st June

211 18:00-24:00 pm were excluded from P2, because they were highly affected by near-site

212 biomass burning emission (detailed information is provided in Section 3.3).

213 **3.2 Concentrations of PM$_{2.5}$, OC, EC, WSOC and WIOC**

214   Concentrations of PM$_{2.5}$ and carbonaceous components are presented in Table 1.

215 PM$_{2.5}$ concentrations range from 21 to 395 μg m^{-3} with a mean value at 159 ± 89 μg

216 m^{-3} during the whole sampling period. As shown in Figure 2, PM$_{2.5}$ concentrations in

217 P1 (average $\pm$ 1σ $= 231\pm89$ μg m^{-3}) increase continuously from around 150 μg

218 m^{-3} to higher than 300 μg m^{-3}, indicating the occurrence of a severe air pollution

219 episode. In contrast, PM$_{2.5}$ concentration during P2 is as low as 43 ± 14 μg m^{-3}.

220 Similarly, the average concentration of OC is 29.4 ± 7.8 μg m^{-3} in P1, which is more

221 than 5 time higher than that in P2 (5.5 ± 1.7 μg m^{-3}) . EC concentrations also decrease

222 dramatically from P1 (12.1 ± 4.0 μg m^{-3}) to P2 (1.5 ± 1.5 μg m^{-3}). The average

223 OC/EC ratio is 3.0 ± 0.9 for the whole sampling period, but the ratio in P2 (3.8 ± 1.0)

224   is higher than that in P1 (2.5±0.4), mainly due to the high SOA formation activities

225   in the rural areas of NCP in summer. It's worthwhile to note that the average OC/EC

226   ratio during the BB-influenced P1 is much lower than the results reported for wheat

227   straw burning in combustion chamber (12.9 ± 2.1) (Tian et al., 2017) and residential

228   stove (6.3-11.1) (Li et al., 2009). The first reason is that fossil fuel burning (such as

229   coal burning and vehicle exhaust) with lower OC/EC ratio (Tian et al., 2017) are still

230   important sources in the region, which are also discussed in Section 3.4. On the other

231   hand, this phenomenon may also be related to different combustion conditions of

232   agricultural residuals in the open field. Li et al. (2009) found that the flaming fire

233   from biomass burning would result in more EC emission and lower OC/EC ratio

234   compared to smoldering fire. Actually, Hays et al. (2005) obtained similar low OC/EC

235   ratio of 2.4 for open wheat straw burning smoke from Washington, US. Thus, the

236   lower ratio of OC/EC observed in this work may indicate that wheat straw

237   combustion in NCP during P1 mainly occurred in the flaming phase.

238   As shown in Figure 2 and 3, the concentrations of WSOC show a consistent

239   temporal variation as those of OC (R^2=0.82), highlighting the fact that WSOC is an

240   important fraction of OC in this region. In addition, the average ratio of WSOC/OC is

241   higher during P1 (0.62±0.16) than during P2 (0.48±0.12), mainly due to enhanced

242   emissions of water-soluble organic compounds (such as sugars, fatty alcohols/acids)

243   from biomass burning during P1. Due to the removal effect of the intermittent raining,

244   concentrations of water-insoluble OC in P2 (3.0±1.3 µg m^{-3}) are also much lower

245   than those in P1 (10.3±4.4 µg m^{-3}).

246   The diurnal variation profiles of EC/OC and WSOC/OC are shown in Figure 4.

247   EC/OC is generally lower in daytime and the lowest value occur during 12:00-15:00

248   pm, mainly due to enhanced daytime formation of SOC. Previous studies have shown

249   that SOA are mainly composed of water-soluble compounds, e.g.,

250   polyacids/polyalcohols and phenols (Kondo et al., 2007;Wang et al., 2009a).

251   However, these compounds can be emitted from primary emissions as well, especially

252   from biomass burning (Shen et al., 2017;Fu et al., 2012). In this study, the WSOC/OC

253   presents lower value during daytime, especially in the afternoon when photo-chemical

254   oxidation is favorable. In addition, the diurnal variation pattern of WSOC/OC is

255   similar to that of levoglucosan/OC. Given that levoglucosan is a marker of biomass

256   burning emissions (Simoneit et al., 1999;Simoneit et al., 2004a), and many kinds of

257   SOA could be produced in the biomass burning plumes during the long-range

258   transport (detailed discussions are given in Section 3.3). These results indicate that

259   particulate WSOC in the region is mostly derived from biomass burning activities

260   including direct emission and secondary oxidation.

261   **3.3 Organic molecular composition**

262   More than 100 organic species were detected in the aerosol samples, and their

263   concentrations are shown in Table 2 and S1. In this study, these organic compositions

264   are grouped into 10 compound classes based on functional groups and sources. Total

265   concentrations of the measured organics range from 177 to 6248 ng m^{-3} (average =

266   1806$\pm$1308 ng m^{-3}) during the whole sampling period with the predominance of

267   sugar compounds, followed by fatty acids and fatty alcohols. The temporal variation

profiles of the determined organic groups are shown in Figure 5. Nearly all the

measured organic species, especially *n*-alkanes, fatty acids, fatty alcohols, sugar

compounds, and PAHs, show much higher concentrations in P1 than in P2 (Figure

S2), indicating an important influence of regional biomass burning on airborne

organic aerosols in NCP.

3.3.1 Biomass-burning tracers

As described in Section 3.1, intensive emissions of open biomass burning were

observed in the southern part of NCP during June 13-16 (P1), which is an important

reason for the severe regional air pollution during this period. Levoglucosan, which is

produced in large quantities during pyrolysis of cellulose, is a key tracer for biomass

burning emissions (Simoneit, 2002;Simoneit et al., 1999). As shown in Table 2,

levoglucosan is the most abundant single compound in the whole sampling period,

ranged from 5.6 to 1447 ng m^{-3} with a mean concentration of 240 ± 288 ng m^{-3}.

Levoglucosan shows good positive correlations with both OC (R^2=0.61) and WSOC

(R^2=0.65) (Figure 3), confirming that biomass burning is an important source of both

aerosol OC and WSOC in the rural region of NCP during the sampling period. As

clearly shown in Figure 6, the concentrations of levoglucosan present a continual

increasing trend during P1 with a mean value of 404 ± 344 ng m^{-3}. However, the tracer

presents very low concentrations (11-123 ng m^{-3}) for most of the time during Jun 20-

22. Interestingly, the concentration of levoglucosan suddenly increased by more than

10 times at 21st Jun 18:00 pm to approximately 1200 ng m^{-3} within less than 3 hours

and then decreased to its beginning concentration (less than 100 ng m^{-3}) within 6

290   hours (2 samples) afterwards. The concentrations of OC, WSOC and EC also showed

291   obvious peaks during this event. However, based on analyses of back-trajectories

292   (Figure 1c) and wind conditions (Figure S1), no significant change of air mass origins

293   was observed. Also, not all organic markers showed similar variations to

294   levoglucosan. For example, the concentrations of PAHs, hopanes, and phthalate esters

295   changed little during this event. Thus, it is plausible to conclude that this variation

296   was caused by emissions from biomass burning activities nearby the sampling site.

297   For this reason, the data of the 2 samples were excluded from P2.

298   The two isomers of levoglucosan, galactosan and mannosan, are also produced

299   by the pyrolysis of cellulose/hemicelluloses (Simoneit, 2002), and thus also

300   considered as important markers of biomass burning. Similar to levoglucosan, the

301   concentrations of these two anhydrosugars in P1 are 5-6 times higher than those in P2.

302   The isomeric ratios of levoglucosan to other anhydrosugars are considered as good

303   indicators of biomass burning. Fabbri et al. (2009) compared the concentrations of the

304   three anhydrosaccharides in the smokes from different fuel types, and proposed that

305   levoglucan/(galactosan+mannosan) (L/G+M) and levoglucan/mannosan (L/M) values

306   range in 0.2-18 and 0.23-33 for various source tests for biomass burning as compared

307   to the average of 54 and 54 for lignites. As shown in Table 2, average ratios of L/G+M

308   and L/M during P1 (10.1±3.41 and 6.77±1.97, respectively) and P2 (29.7±12.2 and

309   18.0±4.28) suggest that biomass burning is always the dominated contributor for

310   these compounds in the rural area of NCP in summer.

311   **3.3.2 Aliphatic lipid composition**

312   The average concentration of all the n-alkanes (C_{18}–C_{36}) measured in this study

313   is 207 ± 149 ng m^{-3} with the most abundant individual compound being nonacosane

314   (C_{max}=$C_{29}H_{60}$) (Table S1). n-Alkanes derived from terrestrial plants are dominated by

315   high molecular weight species (HMW, carbon number >25) with an odd number

316   preference. In contrast, fossil fuel derived n-alkanes do not have odd/even number

317   preference (Rogge et al., 1993a;Simoneit et al., 2004b). In general, n-alkanes with a

318   carbon preference index (CPI, odd/even) more than 5 are considered as plant wax,

319   while those with a CPI nearly unity are mostly derived from fossil fuel combustion

320   (Rogge et al., 1993a, b). In this study, the mean value of CPI is 2.47 ± 1.12, indicating

321   that both fossil fuel and plant wax contribute to n-alkanes in the rural areas of NCP in

322   summer. However, n-alkanes show a stronger odd/even carbon number predominance

323   in P1 (CPI=2.85) than in P2 (CPI=1.64). In addition, all the low molecular weight n-

324   alkanes (LMW, carbon number <25) present a higher contribution to total n-alkanes in

325   P2 than in P1 (Figure 7 a and d). These results demonstrate that plant waxes from

326   biomass burning emissions made a bigger contribution to organic aerosols in the

327   sampling region during P1.

328   A homologous series of 19 saturated fatty acids ($C_{12:0}$–$C_{32:0}$) and 3 unsaturated

329   fatty acids ($C_{16:1}$, $C_{18:1}$, and $C_{18:2}$) were detected (Table S1), and their total

330   concentration is 514 ± 384 ng m^{-3} during the whole period. A strong even carbon

331   number predominance is observed with C_{max} at $C_{28:0}$ and $C_{16:0}$ (Table S1). Higher

332   molecular weight (HMW) fatty acids ($\geq C_{20}$) are derived from terrestrial plant waxes,

333   while LMW fatty acids ($\leq C_{19}$) have multiple sources such as vascular plants,

334 microbes and marine phytoplankton as well as kitchen emissions (Rogge et al.,

335 1993b;Kawamura et al., 2003). The total concentrations of fatty acids present similar

336 temporal variation to levoglucosan with a robust linear correlation (R^2=0.72) (Figure

337 8a), indicating that fatty acids are mostly affected by biomass burning emission

338 during the whole sampling period. Still, there are some evidences that regional

339 emission from wheat straw burning significantly affected the distribution of fatty

340 acids in the aerosols of Gucheng during P1. Firstly, the total concentrations of fatty

341 acids in P1 (900 ± 358 ng m^{-3}) are more than 6 times higher than those in P2 (145 ± 48

342 ng m^{-3}). Secondly, the concentrations and relative contributions of HMW fatty acids

343 ($C_{20:0}$–$C_{32:0}$) are much higher in P1 than in P2, similar to the results of n-alkanes. In

344 addition, the mean value of CPI of HMW fatty acids in P1 (4.21 ± 1.14) is also higher

345 than that in P2 (3.50 ± 1.64).

346   Fatty alcohols in the range of C_{22}−C_{30} were detected for the PM$_{2.5}$ samples with a

347 mean concentration of 193 ± 187 ng m^{-3} (Table 2 and S1) during the whole sampling

348 period. Their distributions are characterized by even carbon number predominance

349 with a maximum at C_{28} (Figure 7c and f). The total concentration of fatty alcohols

350 strongly correlates with levoglucosan (R^2=0.73) (Figure 8b), suggesting that they can

351 also be emitted from biomass burning. It is reasonable since HMW fatty alcohols ($\geqslant$

352 C_{20}) abundantly present in higher plants and loess deposits (Wang and Kawamura,

353 2005). Similar to fatty acids, nearly 10 times higher concentration of fatty alcohols is

354 observed in P1 (322 ± 151 ng m^{-3}) compared with those in P2 (34 ± 23 ng m^{-3}).

355 **3.3.3 Primary saccharides**

356   In addition to the three anhydrosugars, 4 primary sugars (fructose, glucose, sucrose

357   and trehalose) and 3 sugar alcohols (arabitol, mannitol and inositol) were detected in

358   the samples. Primary saccharides have been used as biomarkers for primary biota

359   emissions (Wang et al., 2011). Their mean concentrations range from 3.6 to 49 ng m^{-3}

360   during the whole sampling period. In this study, concentrations of fructose, sucrose and

361   trehalose in P1 are 7-10 times higher than those in P2 (Table S1). They well correlate

362   with levoglucosan (R^2=0.47-0.62, Figure S3) during P1, in contrast to P2, during which

363   no relationships are found between them. These results indicate that these primary

364   sugars are also affected by open-field emissions of biomass burning during P1. Sugar

365   alcohols, mainly arabitol and mannitol, are abundant in airborne fungal spores (Graham

366   et al., 2002). Some studies suggested that biomass burning activities can enhance the

367   emission of sugar alcohols at a certain level (Engling et al., 2009;Fu et al., 2012;Yang

368   et al., 2012). However, no significant relationship (R^2<0.10) can be found between

369   these sugar alcohols and levoglucosan even in P1, indicating the negligible contribution

370   of biomass burning to the tracers in this study.

371   **3.3.4 PAHs, Hopanes and Phthalates**

372   As shown in Figure 5, the temporal variation of PAHs, hopanes, and phthalate

373   esters were clearly different from those of the molecular tracers for biomass burning,

374   especially in P1. In contrast to the continuous increase of sugars, fatty acids, fatty

375   alcohols, and n-alkanes during P1, the concentrations of PAHs, hopanes, and phthalate

376   esters show obvious day-night variations, indicating that biomass burning activities

377   contribute little on these species. Phthalates are widely used as plasticizers in synthetic

378 polymers or softeners in polyvinylchlorides (PVC) (Simoneit et al., 2004b) and can be

379 directly emitted from the matrix into the air as they are not chemically bonded with the

380 matrix. Six phthalate esters were detected in the sampling aerosols, i.e., dimethyl

381 (DMP), diethyl (DEP), diisobutyl (DiBP), butyl isobutyl (BiBP), di-n-butyl (DnBP),

382 and bis(2-ethylhexyl) (BEHP) phthalates (Table S1). The concentrations of total

383 detected phthalate esters in P1 (112 ± 33 ng m^{-3}) are around 2 times only higher than

384 those in P2 (51 ± 18 ng m^{-3}). Hopanes are abundant in coal and crude oils, and enriched

385 in lubricant oil fraction (Oros and Simoneit, 2000;Kawamura et al., 1995).They can be

386 emitted to the atmosphere from coal burning and/or internal combustion of fuel in

387 engines. Only two dominant hopanes, $17\alpha(H),21\beta(H)$-30-norhopane($C_{29\alpha\beta}$) and

388 $17\alpha(H),21\beta(H)$-hopane($C_{30\alpha\beta}$), were detected in all of the samples in this study. Their

389 average concentration in P1 (4.40 ± 2.48 ng m^{-3}) is ~ 2.5 times of that in P2 ($1.81 \pm$

390 0.31 ng m^{-3}). Considering the much higher concentrations of levoglucosan in P1 (on

391 average ~ 8 times higher than P2), these results again confirm a limited influence of

392 biomass burning on concentrations of phthalate esters and hopanes in the aerosols in

393 the rural region. Thus, there were no significant concentration changes of the two

394 species at 21st Jun 18:00-24:00 pm, when the air masses were highly affected by nearby

395 biomass burning activities.

396 PAHs are the products of incomplete combustion of carbon-containing materials

397 and are of high toxicity and carcinogenicity (Halek et al., 2008;Sultan et al., 2001).

398 Previous studies indicated that PAHs are mainly emitted from coal burning and vehicle

399 exhaust in most areas of China (Wang et al., 2006a). However, it has been reported that

combustion of biomass materials can also contribute to the PAHs in the atmosphere (Simoneit, 2002;Ge et al., 2012;Young et al., 2016). In this study, PAH has no significant correlation with levoglucosan during the whole sampling period. Yet the concentrations of total PAHs in P1 (18.6 ± 11 ng m^{-3}) are nearly 8 times higher than those in P2 (2.3 ± 1.0 ng m^{-3}). These results suggest that although the emission of biomass burning is not the most important source for PAHs during the entire period, the intensive regional burning of wheat straw in P1 can also enhance the PAHs concentration in the atmosphere of Gucheng.

As shown in Figure 9, all the primary aerosol markers mentioned above show lower concentrations in daytime with lowest concentrations at afternoon (12:00-18:00 pm), in consistent with the favorable dispersion conditions caused by high temperature and planetary boundary layer (PBL) height. However, the day-night variation of PAHs, hopanes, and phthalate esters are more obvious than other species, again confirming the lower contribution of biomass burning to these organic compositions.

3.3.5 Secondary organic aerosols (SOA) tracers

Eight compounds were identified as isoprene oxidation products in the PM$_{2.5}$ samples, including two methyltetrahydrofuran diols, three C$_5$-alkene triols, two 2-methyltetrols, and 2-methylglyceric acid (Table S1). Detailed information about formation and contribution of these compositions were discussed in our previous paper (Li et al., 2018). The concentrations of total detected isoprene-derived products are 112 ± 86 ng m^{-3}, with much higher concentration in P1 (209 ± 105 ng m^{-3}) than in P2 (57 ± 29 ng m^{-3}).

cis-Pinonic acid (PNA), pinic acid (PA), 3-hydroxyglutaric acid (HGA) and 3-methyl-1,2,3-butanetricarboxylic acid (MBTCA) were detected as tracers for α-/β-pinene oxidation in this study, and their concentrations are shown in Table S1. The concentration of total detected α-/β-pinene oxidation tracers is 66 ± 31 ng m^{-3}, with MBTCA (31 ± 14 ng m^{-3}) being the major compound during the whole sampling period. PNA and PA are considered as first-generation products of α-/β-pinene oxidation. They can be produced by further oxidation of carbonyl-substituted Criegee intermediates formed by α-pinene ozonolysis (Jenkin et al., 2000;Ma et al., 2008), or by OH oxidation of α-pinene under NO$_X$ free conditions (Eddingsaas et al., 2012;Xuan et al., 2015). The formation of 3-HGA is supposed to be based on a ring opening mechanism and may be related to a heterogeneous reaction of these monoterpenes with irradiation in the presence of NOx (Jaoui et al., 2005;Claeys et al., 2007). As shown in Figure 6b-d, PNA, PA and HGA present similar temporal variations and correlated well each other (R^2=0.48-0.76, Figure S4). The formation of MBTCA is explained by further photodegradation of cis-pinonic acid and pinic acid with OH radical (Müller et al., 2012;Szmigielski et al., 2007). As a later-generation oxidation products, MBTCA show an obviously different temporal variation profile than those of PNA and PA, and has no significant increase during P1. In addition, the concertations of PNA, PA and HGA in P1 are 2-8 times higher than those in P2. However, the concentrations of MBTCA in the two periods are comparable. These results are consistent with the longer time scales of formation pathway, lower volatility and longer lifetime of MBTCA in the atmosphere compared to the first-generation products of α-/β-pinene oxidation. β-Caryophyllinic

acid, formed either by ozonolysis or photo-oxidation of β-caryophyllene (a sesquiterpene) (Jaoui et al., 2007), was also determined in this study, and its concentration range from 0.49 to 78 ng m^{-3} (Ave. 17±17 ng m^{-3}). The mean concentration of β-caryophyllinic acid in P1 is 35±21 ng m^{-3}, being 5 times higher than that in P2 (4.1±1.2 ng m^{-3}).

Undoubtedly, the combustion of biomass materials can release a large amount of VOCs, including isoprene and terpenoids (Andreae and Merlet, 2001). As shown in Figure 5 and 6, total biogenic SOA tracers, the sum of detected tracers of isoprene, α-/β-pinene, and β-caryophyllene derived SOA, show a similar temporal variation pattern as levoglucosan with a moderate correlation (R^2=0.56, Figure S5a). Specifically, levoglucosan shows strong linearly correlations with 3-hydroxyglutaric acid (R^2=0.72) (Figure 8c) and β-caryophyllinic acid (R^2=0.80) (Figure 8d), indicating a significant contribution of biomass burning emissions to the formation of SOA derived from mono- and sesqui- terpene oxidation. In our previous paper (Li et al., 2018), we discussed the different diurnal variations of isoprene-derived SOA tracers. In this study, the diurnal variations of other SOA tracers are shown in Figure 10. All the SOA tracers present weaker day-night variations compared to primary organic aerosol markers, because of the competition between the enhanced daytime formation by photoxidation and the nighttime accumulation associated with a low PBL. Yet, there are some differences between these SOA tracers. For example, PNA and PA present lowest concentrations in the afternoon (12:00-18:00 pm) due to their relatively high volatilities, which is unfavorable for gas-to-particle phase partitioning. However, the later-generation

product of PNA and PA, i.e., the less volatile MBTCA, continuously increases during the daytime.

Two classes of aromatic SOA markers, phthalic acids and 2,3-dihydroxy-4-oxopentanoic acid (DHOPA), were detected in the samples as well. Phthalic acids are believed to be produced by the oxidation of naphthalene and other PAHs (Kawamura et al., 2005;Kawamura and Ikushima, 1993;Kanakidou et al., 2005). The mean concentrations of total phthalic acids in the whole sampling period range from 17 to 487 ng m^{-3} with a mean value of 155±94 ng m^{-3}. Their different temporal variation patterns than levoglucosan suggest that biomass burning emission contributes little to phthalic acids formation in the region. The DHOPA was considered to be a tracer compound for toluene-derived SOA (Kleindienst et al., 2004). DHOPA presents a similar temporal variation and a moderate correlation with levoglusoan (R^2=0.51, Figure S5b), indicating a certain contribution of biomass burning. Similar to MBTCA, the volatility of DHOPA is quite low, and thus mainly exists in the particle phase at field temperature (Ding et al., 2017). Thus, DHOPA shows a similar diurnal variation to MBTCA, with higher concentrations during daytime.

3.4 Assessment of source contributions

In order to investigate the differences in organic aerosol sources between the two representative periods, we classified all the measured organic compounds into seven different sources: (a) "plant emission" represented by higher plant wax n-alkanes, HMW fatty acids and fatty alcohols ($\geq$C$_{20}$); (b) "fossil fuel combustion" mainly represented by fossil fuel derived n-alkanes, hopanes, and PAHs; (c) "biomass burning"

488 represented by levoglucosan and its isomers; (d) "marine/microbial source" represented

489 by LMW fatty acids ($<C_{20}$); (e) "soil/fungal spore/pollen" represented by primary

490 saccharides and sugar alcohols; (f) "plastic emission" represented by phthalate esters;

491 and (g) "secondary oxidation" represented by biogenic SOA tracers, DHOPA, and

492 phthalic acids. The concentrations of individual classes and their contributions to OC

493 content during P1 and P2 are summarized in Figure 11. Plant emission-derived

494 compounds accounted for a larger fraction of $PM_{2.5}$ OC during P1 than during P2 (mean

495 fractions of $28.7 \pm 9.3‰$ in P1 vs. $16.5 \pm 7.2‰$ in P2). The average faction of biomass

496 burning-derived organics in P1 ($6.0 \pm 3.9‰$) is also higher than that in P2 ($4.6 \pm 2.1‰$),

497 so do organics derived from soil/fungal spore/pollen. However, organic molecules from

498 the other 4 sources present a higher contribution to OC in P2 than in P1.

499 Since organic compounds in the $PM_{2.5}$ samples cannot be completely determined

500 and some of them are of different sources, thus the above classification based on the

501 measured compounds could result in certain uncertainty in assessing source

502 contributions (Simoneit et al., 2004b). Here, we further used a tracer-based source

503 apportionment method to quantitatively estimate the contributions of primary and

504 secondary sources to the fine particulate OC at the rural site. As described above, two

505 samples collected at 21st Jun 18:00-24:00 pm were considered to be highly affected by

506 the direct emission from biomass burning nearby the sampling site. Thus, the average

507 OC/levoglucosan ratio in the smoke of biomass burning ($\left(\frac{OC}{Levo}\right)_{BB}$) can be estimated

508 by using the following equation:

509 $$\left(\frac{OC}{Levo}\right)_{BB} = \frac{OC_n - \frac{1}{2}(OC_{before} + OC_{after})}{Levo_n - \frac{1}{2}(Levo_{before} + Levo_{Levo})}$$ (E1)

510   where OC_n and $Levo_n$ are the average concentrations of OC and levoglucosan in

511 the two PM$_{2.5}$ samples affected by the nearby sources. OC_{before} and $Levo_{before}$ are the

512 concentrations of OC and levoglucosan in the samples collected before the event, while

513 OC_{after} and $Levo_{after}$ are the concentrations of OC and levoglucosan in the samples

514 collected after the event. The mean values in the "before" and the "after" samples were

515 subtracted to minimize the influence of local background contribution. The calculated

516 $\left(\frac{OC}{Levo}\right)_{BB}$ in this study is 18.7, which is somewhat higher than the average value of 12.1

517 measured in PM$_{2.5}$ aerosols emitted from the burning of three types of cereal straws

518 (i.e., wheat, maize, and rice) in China (Zhang et al., 2007b). This difference can be

519 attributed to the differences of burning conditions. For other sources, the measured

520 concentrations of mannitol were used to calculate the contributions of fungal spores to

521 OC (Bauer et al., 2008), and SOA tracers were used to estimate the SOC formed from

522 the oxidation of isoprene, α-/β-pinene, β-caryophyllene, and toluene (Kleindienst et al.,

523 2007). Also, these tracer-based approaches tend to have large uncertainties, especially

524 for SOC estimation (Li et al., 2013a). However, our results are still meaningful to

525 understand the relative abundances of organic aerosols from these sources in different

526 periods.

527   As shown in Figure 12, biomass-burning derived OC, ranging from 0.11-27.5 μgC

528 m^{-3}, is the dominant source, which accounts for 1.16-74.8% (ave. 22.6%) of OC in the

529 aerosols of the rural region during the whole sampling period. Fungal-spore derived OC

530 (0.003-5.12 μgC m^{-3}) is a minor source, only accounting for 0.43% (0.003-5.12%) of

531 OC. The contribution of total SOC derived from oxidation of isoprene, α-/β-pinene, β-

532 caryophyllene, and toluene to OC ranged from 5.90-34.1% with an average of 16.7%.

533 Among the four SOC precursors, toluene-derived products account for 7.78% (2.06-

534 21.7%) of OC, being the most important SOC contributor. The relative abundances of

535 these sources show clear temporal variations during the whole sampling period (Figure

536 12). The contribution of biomass burning derived OC to total OC in P1 (27.6%) is 1.7

537 times of that in P2 (17.1%) (Figure 13), further indicating the strong regional impact of

538 open-field wheat straw burning on the molecular compositions of organic aerosols in

539 the rural area of NCP. The contribution of SOC from oxidation of the four VOCs

540 increase slightly from P1 (16.3%) to P2 (21.1%). It should be noted that biomass

541 burning can also release a large amount of VOCs, which may produce more secondary

542 organic aerosols during the long-range transport. Thus, the impact of intensive biomass

543 burning in the southern region of NCP on organic aerosols in the Gucheng area is likely

544 even stronger than the estimation presented above with implications for regional

545 climate.

546 **4. Summary and Conclusion**

547 During the entire sampling period, OC and WSOC showed strong positive

548 correlations with levoglucosan, and the diurnal variation of WSOC/OC was similar to

549 that of levoglucosan/OC, suggesting that summertime organic aerosols in the rural

550 area of NCP are highly affected by direct emission of BB. Higher relative abundances

551 and CPI values of HMW n-alkanes, fatty acids and fatty alcohols in P1 indicated an

552 enhanced effect of open-field biomass burning on molecular composition of organic

aerosols. PAHs, hopanes, and phthalate esters presented different temporal and diurnal

variations to levoglucosan because of the lower contribution of BB to these organic

compositions. The total biogenic SOA tracers showed a similar temporal variation and

a moderate correlation with levoglucosan, demonstrating the enhancing effect of BB

emission on BSOA formation. Later-generation SOA products, e.g., MBTCA in this

study, were unlikely affected directly by BB emission, and thus showed little changes

in concentrations between the two periods. The source distribution results derived

using a tracer-based method demonstrated that the contribution of BB to organic

aerosols increased by more than 50% during the period influenced by regional open-

field biomass burning (P1) compared to the period when local emissions were more

dominant (P2). However, this contribution may even be underestimated since BB can

also release a large amount of VOCs enhancing the formation of SOA in the

atmosphere. Our results confirmed that intensive field burning of biomass fuels can

significantly influence the concentration and composition of aerosols, and thus affect

atmospheric chemistry and climate on a regional scale.

Author Contributions
G.H. Wang designed the experiment. G.H. Wang, T. Zhu and L.M. Zeng arranged the
sample collection. J.J. Li. and G.H. Wang collected the samples. J.J. Li, G.H. Wang, J.
Li, C. Wu and W.Q. Jiang analyzed the samples. J.J. Li, and G.H. Wang performed the
data interpretation. J.J. Li, G.H. Wang and Q. Zhang wrote the paper.

Acknowledgements
This work was financially supported by the program from National Nature Science
Foundation of China (No. 41773117, 91543116, 41405122). The authors gratefully
acknowledge the use of fire spots data products from the Land, Atmosphere Near real-
time Capability for EOS (LANCE) system operated by the NASA/GSFC/Earth

581 Science Data and Information System (ESDIS) with funding provided by NASA/HQ
582 (https://firms.modaps.eosdis.nasa.gov/firemap/), and the NOAA Air Resources
583 Laboratory (ARL) for the provision of the HYSPLIT transport and dispersion model
584 and/or READY website (http://www.ready.noaa.gov) used in this publication.

585
586
587

Reference

589 Aggarwal, S. G., Kawamura, K., Umarji, G. S., Tachibana, E., Patil, R. S., and Gupta, P. K.: Organic and
590   inorganic markers and stable C-, N-isotopic compositions of tropical coastal aerosols from megacity
591   Mumbai: sources of organic aerosols and atmospheric processing, Atmos. Chem. Phys., 13, 4667-
592   4680, 10.5194/acp-13-4667-2013, 2013.

593 Andreae, M. O., and Merlet, P.: Emission of trace gases and aerosols from biomass burning, Global
594   Biogeochemical Cycles, 15, 955-966, 10.1029/2000gb001382, 2001.

595 Andreae, M. O., and Rosenfeld, D.: Aerosol–cloud–precipitation interactions. Part 1. The nature and
596   sources of cloud-active aerosols, Earth-Science Reviews, 89, 13-41,
597   10.1016/j.earscirev.2008.03.001, 2008.

598 Chan, M. N., Choi, M. Y., Ng, N. L., and Chan, C. K.: Hygroscopicity of water-soluble organic
599   compounds in atmospheric aerosols: Amino acids and biomass burning derived organic species,
600   Environ. Sci. Technol., 39, 1555-1562, 10.1021/es049584l, 2005.

601 Claeys, M., Szmigielski, R., Kourtchev, I., Van der Veken, P., Vermeylen, R., Maenhaut, W., Jaoui, M.,
602   Kleindienst, T. E., Lewandowski, M., Offenberg, J. H., and Edney, E. O.: Hydroxydicarboxylic
603   Acids: Markers for Secondary Organic Aerosol from the Photooxidation of α-Pinene, Environ. Sci.
604   Technol., 41, 1628-1634, 10.1021/es0620181, 2007.

605 Dinar, E., Anttila, T., and Rudich, Y.: CCN activity and hygroscopic growth of organic aerosols following
606   reactive uptake of ammonia, Environ. Sci. Technol., 42, 793-799, 10.1021/es071874p, 2008.

607 Ding, X., Zhang, Y. Q., He, Q. F., Yu, Q. Q., Wang, J. Q., Shen, R. Q., Song, W., Wang, Y. S., and Wang,
608   X. M.: Significant Increase of Aromatics-Derived Secondary Organic Aerosol during Fall to Winter
609   in China, Environ. Sci. Technol., 51, 7432-7441, 10.1021/acs.est.6b06408, 2017.

610 Eddingsaas, N. C., Loza, C. L., Yee, L. D., Chan, M., Schilling, K. A., Chhabra, P. S., Seinfeld, J. H., and
611   Wennberg, P. O.: alpha-pinene photooxidation under controlled chemical conditions - Part 2: SOA
612   yield and composition in low- and high-NOx environments, Atmos. Chem. Phys., 12, 7413-7427,
613   10.5194/acp-12-7413-2012, 2012.

614 Engling, G., Lee, J. J., Tsai, Y. W., Lung, S. C. C., Chou, C. C. K., and Chan, C. Y.: Size-Resolved
615   Anhydrosugar Composition in Smoke Aerosol from Controlled Field Burning of Rice Straw,
616   Aerosol Science and Technology, 43, 662-672, 10.1080/02786820902825113, 2009.

617 Fabbri, D., Torri, C., Simoneit, B. R. T., Marynowski, L., Rushdi, A. I., and Fabiańska, M. J.:
618   Levoglucosan and other cellulose and lignin markers in emissions from burning of Miocene lignites,
619   Atmos. Environ., 43, 2286-2295, 2009.

620 Fu, P. Q., Kawamura, K., Pavuluri, C. M., Swaminathan, T., and Chen, J.: Molecular characterization of
621   urban organic aerosol in tropical India: contributions of primary emissions and secondary
622   photooxidation, Atmos. Chem. Phys., 10, 2663-2689, 2010.

623 Fu, P. Q., Kawamura, K., Chen, J., Li, J., Sun, Y. L., Liu, Y., Tachibana, E., Aggarwal, S. G., Okuzawa,
624   K., Tanimoto, H., Kanaya, Y., and Wang, Z. F.: Diurnal variations of organic molecular tracers and

stable carbon isotopic composition in atmospheric aerosols over Mt. Tai in the North China Plain: an influence of biomass burning, Atmos. Chem. Phys., 12, 8359-8375, 10.5194/acp-12-8359-2012, 2012.

Ge, X., Setyan, A., Sun, Y., and Zhang, Q.: Primary and secondary organic aerosols in Fresno, California during wintertime: Results from high resolution aerosol mass spectrometry, Journal of Geophysical Research: Atmospheres, 117, n/a-n/a, 10.1029/2012jd018026, 2012.

Graham, B., Mayol-Bracero, O. L., Guyon, P., Roberts, G. C., Decesari, S., Facchini, M. C., Artaxo, P., Maenhaut, W., Koll, P., and Andreae, M. O.: Water-soluble organic compounds in biomass burning aerosols over Amazonia - 1. Characterization by NMR and GC-MS, J. Geophys. Res.-Atmos., 107, DOI:804710.801029/802001jd000336, 2002.

Guo, S., Hu, M., Zamora, M. L., Peng, J., Shang, D., Zheng, J., Du, Z., Wu, Z., Shao, M., Zeng, L., Molina, M. J., and Zhang, R.: Elucidating severe urban haze formation in China, Proceedings of the National Academy of Sciences of the United States of America, 111, 17373-17378, 10.1073/pnas.1419604111, 2014.

Halek, F., Nabi, G., and Kavousi, A.: Polycyclic aromatic hydrocarbons study and toxic equivalency factor (TEFs) in Tehran, IRAN, Environmental Monitoring and Assessment, 143, 303-311, 10.1007/s10661-007-9983-9, 2008.

Hallquist, M., Wenger, J. C., Baltensperger, U., Rudich, Y., Simpson, D., Claeys, M., Dommen, J., Donahue, N. M., George, C., Goldstein, A. H., Hamilton, J. F., Herrmann, H., Hoffmann, T., Iinuma, Y., Jang, M., Jenkin, M. E., Jimenez, J. L., Kiendler-Scharr, A., Maenhaut, W., McFiggans, G., Mentel, T. F., Monod, A., Prevot, A. S. H., Seinfeld, J. H., Surratt, J. D., Szmigielski, R., and Wildt, J.: The formation, properties and impact of secondary organic aerosol: current and emerging issues, Atmos. Chem. Phys., 9, 5155-5236, 2009.

Hays, M. D., Fine, P. M., Geron, C. D., Kleeman, M. J., and Gullett, B. K.: Open burning of agricultural biomass: Physical and chemical properties of particle-phase emissions, Atmos. Environ., 39, 6747-6764, https://doi.org/10.1016/j.atmosenv.2005.07.072, 2005.

Huang, R. J., Zhang, Y. L., Bozzetti, C., Ho, K. F., Cao, J. J., Han, Y. M., Daellenbach, K. R., Slowik, J. G., Platt, S. M., Canonaco, F., Zotter, P., Wolf, R., Pieber, S. M., Bruns, E. A., Crippa, M., Ciarelli, G., Piazzalunga, A., Schwikowski, M., Abbaszade, G., Schnelle-Kreis, J., Zimmermann, R., An, Z. S., Szidat, S., Baltensperger, U., El Haddad, I., and Prevot, A. S. H.: High secondary aerosol contribution to particulate pollution during haze events in China, Nature, 514, 218-222, 10.1038/nature13774, 2014.

Jaoui, M., Kleindienst, T. E., Lewandowski, M., Offenberg, J. H., and Edney, E. O.: Identification and quantification of aerosol polar oxygenated compounds bearing carboxylic or hydroxyl groups. 2. Organic tracer compounds from monoterpenes, Environ. Sci. Technol., 39, 5661-5673, 10.1021/es048111b, 2005.

Jaoui, M., Lewandowski, M., Kleindienst, T. E., Offenberg, J. H., and Edney, E. O.: β-caryophyllinic acid: An atmospheric tracer for β-caryophyllene secondary organic aerosol, Geophysical Research Letters, 34, doi:10.1029/2006GL028827, 2007.

Jenkin, M. E., Shallcross, D. E., and Harvey, J. N.: Development and application of a possible mechanism for the generation of cis -pinic acid from the ozonolysis of α - and β -pinene, Atmos. Environ., 34, 2837-2850, 2000.

Jimenez, J. L., Canagaratna, M. R., Donahue, N. M., Prevot, A. S. H., Zhang, Q., ., Kroll, J. H., Decarlo, P. F., Allan, J. D., Coe, H., ., and Ng, N. L.: Evolution of organic aerosols in the atmosphere, Science,

326, 1525-1529, 2009.

Kanakidou, M., Seinfeld, J. H., Pandis, S. N., Barnes, I., Dentener, F. J., Facchini, M. C., Van Dingenen, R., Ervens, B., Nenes, A., Nielsen, C. J., Swietlicki, E., Putaud, J. P., Balkanski, Y., Fuzzi, S., Horth, J., Moortgat, G. K., Winterhalter, R., Myhre, C. E. L., Tsigaridis, K., Vignati, E., Stephanou, E. G., and Wilson, J.: Organic aerosol and global climate modelling: a review, Atmos. Chem. Phys., 5, 1053-1123, 2005.

Kawamura, K., and Ikushima, K.: Seasonal changes in the distribution of dicarboxylic acids in the urban atmosphere, Environ. Sci. Technol., 27, 2227-2235, 1993.

Kawamura, K., Kosaka, M., and Sempere, R.: Distributions and seasonal changes in hydrocarbons in urban aerosols and rain waters, Chikyu Kagaku (Geochemistry), 29, 1-15 (In Japanese), 1995.

Kawamura, K., Ishimura, Y., and Yamazaki, K.: Four years' observations of terrestrial lipid class compounds in marine aerosols from the western North Pacific, Global Biogeochemical Cycles, 17, 10.1029/2001gb001810, 2003.

Kawamura, K., Imai, Y., and Barrie, L. A.: Photochemical production and loss of organic acids in high Arctic aerosols during long-range transport and polar sunrise ozone depletion events, Atmos. Environ., 39, 599-614, 10.1016/j.atmosenv.2004.10.020, 2005.

Kleindienst, T. E., Conver, T. S., McIver, C. D., and Edney, E. O.: Determination of secondary organic aerosol products from the photooxidation of toluene and their implications in ambient PM2.5, J. Atmos. Chem., 47, 79-100, 2004.

Kleindienst, T. E., Jaoui, M., Lewandowski, M., Offenberg, J. H., Lewis, C. W., Bhave, P. V., and Edney, E. O.: Estimates of the contributions of biogenic and anthropogenic hydrocarbons to secondary organic aerosol at a southeastern US location, Atmos. Environ., 41, 8288-8300, 10.1016/j.atmosenv.2007.06.045, 2007.

Kondo, Y., Miyazaki, Y., Takegawa, N., Miyakawa, T., Weber, R. J., Jimenez, J. L., Zhang, Q., and Worsnop, D. R.: Oxygenated and water-soluble organic aerosols in Tokyo, Journal of Geophysical Research, 112, doi: 10.1029/2006jd007056, 10.1029/2006jd007056, 2007.

Lelieveld, J., Evans, J. S., Fnais, M., Giannadaki, D., and Pozzer, A.: The contribution of outdoor air pollution sources to premature mortality on a global scale, Nature, 525, 367-371, 10.1038/nature15371, 2015.

Li, J. J., Wang, G. H., Cao, J. J., Wang, X. M., and Zhang, R. J.: Observation of biogenic secondary organic aerosols in the atmosphere of a mountain site in central China: temperature and relative humidity effects, Atmos. Chem. Phys., 13, 11535-11549, 10.5194/acp-13-11535-2013, 2013a.

Li, J. J., Wang, G. H., Wang, X. M., Cao, J. J., Sun, T., Cheng, C. L., Meng, J. J., Hu, T. F., and Liu, S. X.: Abundance, composition and source of atmospheric PM 2.5 at a remote site in the Tibetan Plateau, China, Tellus B, 65, doi:10.3402/tellusb.v3465i3400.20281, 2013b.

Li, J. J., Wang, G. H., Wu, C., Cao, C., Ren, Y. Q., Wang, J. Y., Li, J., Cao, J. J., Zeng, L. M., and Zhu, T.: Characterization of isoprene-derived secondary organic aerosols at a rural site in North China Plain with implications for anthropogenic pollution effects, Scientific reports, 8, DOI: 10.1038/s41598-41017-18983-41597, 10.1038/s41598-017-18983-7, 2018.

Li, W. J., Shao, L. Y., and Buseck, P. R.: Haze types in Beijing and the influence of agricultural biomass burning, Atmos. Chem. Phys., 10, 8119-8130, 10.5194/acp-10-8119-2010, 2010.

Li, X., Wang, S., Duan, L., Hao, J., and Nie, Y.: Carbonaceous Aerosol Emissions from Household Biofuel Combustion in China, Environ. Sci. Technol., 43, 6076-6081, 10.1021/es803330j, 2009.

Li, Y. J., Sun, Y., Zhang, Q., Li, X., Li, M., Zhou, Z., and Chan, C. K.: Real-time chemical

characterization of atmospheric particulate matter in China: A review, Atmos. Environ., 158, 270-304, 10.1016/j.atmosenv.2017.02.027, 2017.

Li, Z. Q., Xia, X. G., Cribb, M., Mi, W., Holben, B., Wang, P. C., Chen, H. B., Tsay, S. C., Eck, T. F., Zhao, F. S., Dutton, E. G., and Dickerson, R. R.: Aerosol optical properties and their radiative effects in northern China, J. Geophys. Res.-Atmos., 112, 10.1029/2006jd007382, 2007.

Müller, L., Reinnig, M. C., Naumann, K. H., Saathoff, H., Mentel, T. F., Donahue, N. M., and Hoffmann, T.: Formation of 3-methyl-1,2,3-butanetricarboxylic acid via gas phase oxidation of pinonic acid – a mass spectrometric study of SOA aging, Atmos. Chem. Phys., 12, 1483-1496, 10.5194/acp-12-1483-2012, 2012.

Ma, Y., Russell, A. T., and Marston, G.: Mechanisms for the formation of secondary organic aerosol components from the gas-phase ozonolysis of alpha-pinene, Physical Chemistry Chemical Physics, 10, 4294-4312, 10.1039/b803283a, 2008.

Oros, D. R., and Simoneit, B. R. T.: Identification and emission rates of molecular tracers in coal smoke particulate matter, Fuel, 79, 515-536, http://dx.doi.org/10.1016/S0016-2361(99)00153-2, 2000.

Quan, J. N., Gao, Y., Zhang, Q., Tie, X. X., Cao, J. J., Han, S. Q., Meng, J. W., Chen, P. F., and Zhao, D. L.: Evolution of planetary boundary layer under different weather conditions, and its impact on aerosol concentrations, Particuology, 11, 34-40, 10.1016/j.partic.2012.04.005, 2013.

Rogge, W. F., Hildemann, L. M., Mazurek, M. A., Cass, G. R., and Simoneit, B. R. T.: Sources of Fine Organic Aerosols. 2. Noncatalyst and Catalyst-equipped Automobile and Heavy-duty Diesel Trucks, Environ. Sci. Technol., 27, 636-651, 1993a.

Rogge, W. F., Hildemann, L. M., Mazurek, M. A., Cass, G. R., and Simoneit, B. R. T.: Sources of Fine Organic Aerosols .4. Particulate Abrasion Products from Leaf Surfaces of Urban Plants, Environ. Sci. Technol., 27, 2700-2711, 1993b.

Shen, Z., Zhang, Q., Cao, J., Zhang, L., Lei, Y., Huang, Y., Huang, R. J., Gao, J., Zhao, Z., Zhu, C., Yin, X., Zheng, C., Xu, H., and Liu, S.: Optical properties and possible sources of brown carbon in PM 2.5 over Xi'an, China, Atmos. Environ., 150, 322-330, 10.1016/j.atmosenv.2016.11.024, 2017.

Simoneit, B. R. T., Schauer, J. J., Nolte, C. G., Oros, D. R., Elias, V. O., Fraser, M. P., Rogge, W. F., and Cass, G. R.: Levoglucosan, a tracer for cellulose in biomass burning and atmospheric particles, Atmos. Environ., 33, 173-182, 1999.

Simoneit, B. R. T.: Biomass burning - A review of organic tracers for smoke from incomplete combustion, Applied Geochemistry, 17, 129-162, 2002.

Simoneit, B. R. T., Elias, V. O., Kobayashi, M., Kawamura, K., Rushdi, A. I., Medeiros, P. M., Rogge, W. F., and Didyk, B. M.: Sugars - Dominant water-soluble organic compounds in soils and characterization as tracers in atmospheric particulate matter, Environ. Sci. Technol., 38, 5939-5949, 10.1021/es0403099, 2004a.

Simoneit, B. R. T., Kobayashi, M., Mochida, M., Kawamura, K., Lee, M., Lim, H. J., Turpin, B. J., and Komazaki, Y.: Composition and major sources of organic compounds of aerosol particulate matter sampled during the ACE-Asia campaign, J. Geophys. Res.-Atmos., 109, D19S10, 10.1029/2004jd004598, 2004b.

Sultan, C., Balaguer, P., Terouanne, B., Georget, V., Paris, F., Jeandel, C., Lumbroso, S., and Nicolas, J. C.: Environmental xenoestrogens, antiandrogens and disorders of male sexual differentiation, Molecular and Cellular Endocrinology, 178, 99-105, 10.1016/s0303-7207(01)00430-0, 2001.

Sun, Y. L., Jiang, Q., Wang, Z. F., Fu, P. Q., Li, J., Yang, T., and Yin, Y.: Investigation of the sources and evolution processes of severe haze pollution in Beijing in January 2013, J. Geophys. Res.-Atmos.,

757   119, 4380-4398, 10.1002/2014jd021641, 2014.

758 Sun, Y. L., Jiang, Q., Xu, Y. S., Ma, Y., Zhang, Y. J., Liu, X. G., Li, W. J., Wang, F., Li, J., Wang, P. C.,
759   and Li, Z. Q.: Aerosol characterization over the North China Plain: Haze life cycle and biomass
760   burning impacts in summer, J. Geophys. Res.-Atmos., 121, 2508-2521, 10.1002/2015jd024261,
761   2016.

762 Szmigielski, R., Surratt, J. D., Gomez-Gonzalez, Y., Van der Veken, P., Kourtchev, I., Vermeylen, R.,
763   Blockhuys, F., Jaoui, M., Kleindienst, T. E., Lewandowski, M., Offenberg, J. H., Edney, E. O.,
764   Seinfeld, J. H., Maenhaut, W., and Claeys, M.: 3-methyl-1,2,3-butanetricarboxylic acid: An
765   atmospheric tracer for terpene secondary organic aerosol, Geophysical Research Letters, 34, L24811,
766   10.1029/2007gl031338, 2007.

767 Tian, J., Ni, H. Y., Cao, J. J., Han, Y. M., Wang, Q. Y., Wang, X. L., Chen, L. W. A., Chow, J. C., Watson,
768   J. G., Wei, C., Sun, J., Zhang, T., and Huang, R. J.: Characteristics of carbonaceous particles from
769   residential coal combustion and agricultural biomass burning in China, Atmospheric Pollution
770   Research, 8, 521-527, 10.1016/j.apr.2016.12.006, 2017.

771 Tie, X. X., Huang, R. J., Dai, W. T., Cao, J. J., Long, X., Su, X. L., Zhao, S. Y., Wang, Q. Y., and Li, G.
772   H.: Effect of heavy haze and aerosol pollution on rice and wheat productions in China, Scientific
773   reports, 6, 10.1038/srep29612, 2016.

774 van Donkelaar, A., Martin, R. V., Brauer, M., Kahn, R., Levy, R., Verduzco, C., and Villeneuve, P. J.:
775   Global Estimates of Ambient Fine Particulate Matter Concentrations from Satellite-Based Aerosol
776   Optical Depth: Development and Application, Environmental Health Perspectives, 118, 847-855,
777   10.1289/ehp.0901623, 2010.

778 Venkataraman, C., Habib, G., Eiguren-Fernandez, A., Miguel, A. H., and Friedlander, S. K.: Residential
779   biofuels in south Asia: Carbonaceous aerosol emissions and climate impacts, Science, 307, 1454-
780   1456, 10.1126/science.1104359, 2005.

781 Wang, G. H., and Kawamura, K.: Molecular characteristics of urban organic aerosols from Nanjing: A
782   case study of a mega-city in China, Environ. Sci. Technol., 39, 7430-7438, 10.1021/es051055+,
783   2005.

784 Wang, G. H., Kawamura, K., Lee, S., Ho, K. F., and Cao, J. J.: Molecular, seasonal, and spatial
785   distributions of organic aerosols from fourteen Chinese cities, Environ. Sci. Technol., 40, 4619-
786   4625, 10.1021/es060291x, 2006a.

787 Wang, G. H., Kawamura, K., Watanabe, T., Lee, S. C., Ho, K. F., and Cao, J. J.: High loadings and source
788   strengths of organic aerosols in China, Geophysical Research Letters, 33,
789   L2280110.1029/2006gl027624, 2006b.

790 Wang, G. H., Kawamura, K., Umemoto, N., Xie, M. J., Hu, S. Y., and Wang, Z. F.: Water-soluble organic
791   compounds in PM2.5 and size-segregated aerosols over Mount Tai in North China Plain, J. Geophys.
792   Res.-Atmos., 114, doi: 10.1029/2008jd011390, D1920810.1029/2008jd011390, 2009a.

793 Wang, G. H., Kawamura, K., Xie, M. J., Hu, S. Y., Cao, J. J., An, Z. S., Waston, J. G., and Chow, J. C.:
794   Organic Molecular Compositions and Size Distributions of Chinese Summer and Autumn Aerosols
795   from Nanjing: Characteristic Haze Event Caused by Wheat Straw Burning, Environ. Sci. Technol.,
796   43, 6493-6499, 10.1021/es803086g, 2009b.

797 Wang, G. H., Chen, C. L., Li, J. J., Zhou, B. H., Xie, M. J., Hu, S. Y., Kawamura, K., and Chen, Y.:
798   Molecular composition and size distribution of sugars, sugar-alcohols and carboxylic acids in
799   airborne particles during a severe urban haze event caused by wheat straw burning, Atmos. Environ.,
800   45, 2473-2479, 10.1016/j.atmosenv.2011.02.045, 2011.

Wang, G. H., Zhang, R. Y., Gomez, M. E., Yang, L. X., Zamora, M. L., Hu, M., Lin, Y., Peng, J. F., Guo, S., Meng, J. J., Li, J. J., Cheng, C. L., Hu, T. F., Ren, Y. Q., Wang, Y. S., Gao, J., Cao, J. J., An, Z. S., Zhou, W. J., Li, G. H., Wang, J. Y., Tian, P. F., Marrero-Ortiz, W., Secrest, J., Du, Z. F., Zheng, J., Shang, D. J., Zeng, L. M., Shao, M., Wang, W. G., Huang, Y., Wang, Y., Zhu, Y. J., Li, Y. X., Hu, J. X., Pan, B., Cai, L., Cheng, Y. T., Ji, Y. M., Zhang, F., Rosenfeld, D., Liss, P. S., Duce, R. A., Kolb, C. E., and Molina, M. J.: Persistent sulfate formation from London Fog to Chinese haze, Proceedings of the National Academy of Sciences of the United States of America, 113, 13630-13635, 10.1073/pnas.1616540113, 2016.

Xuan, Z., Renee C, M., Dan D, H., Nathan F, D., Bernard, A., Richard C, F., and John H, S.: Formation and evolution of molecular products in α-pinene secondary organic aerosol, Proceedings of the National Academy of Sciences of the United States of America, 112, 14168-14173, 2015.

Yang, Y. H., Chan, C. Y., Tao, J., Lin, M., Engling, G., Zhang, Z. S., Zhang, T., and Su, L.: Observation of elevated fungal tracers due to biomass burning in the Sichuan Basin at Chengdu City, China, Science of the Total Environment, 431, 68-77, 10.1016/j.scitotenv.2012.05.033, 2012.

Young, D. E., Kim, H., Parworth, C., Zhou, S., Zhang, X., Cappa, C. D., Seco, R., Kim, S., and Zhang, Q.: Influences of emission sources and meteorology on aerosol chemistry in a polluted urban environment: results from DISCOVER-AQ California, Atmos. Chem. Phys., 16, 5427-5451, 10.5194/acp-16-5427-2016, 2016.

Zhang, J. K., Cheng, M. T., Ji, D. S., Liu, Z. R., Hu, B., Sun, Y., and Wang, Y. S.: Characterization of submicron particles during biomass burning and coal combustion periods in Beijing, China, The Science of the total environment, 562, 812-821, 10.1016/j.scitotenv.2016.04.015, 2016.

Zhang, Q., Jimenez, J. L., Canagaratna, M. R., Allan, J. D., Coe, H., Ulbrich, I., Alfarra, M. R., Takami, A., Middlebrook, A. M., and Sun, Y. L.: Ubiquity and dominance of oxygenated species in organic aerosols in anthropogenically-influenced Northern Hemisphere midlatitudes, Geophysical Research Letters, 34, L13801, 2007a.

Zhang, Q., Streets, D. G., Carmichael, G. R., He, K. B., Huo, H., Kannari, A., Klimont, Z., Park, I. S., Reddy, S., Fu, J. S., Chen, D., Duan, L., Lei, Y., Wang, L. T., and Yao, Z. L.: Asian emissions in 2006 for the NASA INTEX-B mission, Atmos. Chem. Phys., 9, 5131-5153, 10.5194/acp-9-5131-2009, 2009.

Zhang, Y., Shao, M., Zhang, Y., Zeng, L., He, L., Zhu, B., Wei, Y., and Zhu, X.: Source profiles of particulate organic matters emitted from cereal straw burnings, Journal of Environmental Sciences, 19, 167-175, https://doi.org/10.1016/S1001-0742(07)60027-8, 2007b.

Zhu, Y., Yang, L., Chen, J., Wang, X., Xue, L., Sui, X., Wen, L., Xu, C., Yao, L., Zhang, J., Shao, M., Lu, S., and Wang, W.: Characteristics of ambient volatile organic compounds and the influence of biomass burning at a rural site in Northern China during summer 2013, Atmos. Environ., 124, 156-165, 10.1016/j.atmosenv.2015.08.097, 2016.

837 Table 1 Concentrations of carbonaceous components in the time-resolved (3-h) PM$_{2.5}$ samples in

838 the rural site of NCP during the whole sampling period, Period 1 (P1) and Period 2 (P2).

Component	Whole period (N=117)			Period 1 (N=28)			Period 2 (N=13)		
	Range	Mean	SD	Range	Mean	SD	Range	Mean	SD
PM$_{2.5}$ (µg m^{-3})	21~395	159	89	133~347	231	59	21~62	43	14
OC (µg m^{-3})	1.7~45.7	17.3	11.1	13.8~44.4	29.4	7.8	3.6~8.8	5.5	1.7
EC (µg m^{-3})	0.2~22.3	6.5	4.9	5.3~22.3	12.1	4.0	0.9~2.6	1.5	0.5
WSOC (µg m^{-3})	0.7~33.0	11.5	8.2	5.3~33.0	19.1	8.3	1.2~4.2	2.6	0.8
WIOC (µg m^{-3})	0.3~28.1	6.4	5.1	4.5~28.1	10.3	4.4	1.2~5.5	3.0	1.3
OC/EC	1.2~7.6	3.0	0.9	1.9~3.2	2.5	0.4	2.5~5.7	3.8	1.0
WSOC/OC	0.07~0.95	0.63	0.18	0.30~0.85	0.62	0.16	0.18~0.67	0.48	0.12
WIOC/OC	0.05~0.93	0.37	0.18	0.15~0.70	0.38	0.16	0.33~0.82	0.52	0.12

839
840
841

842 Table 2 Average concentrations of the organic compound classes (ng m^{-3}) in the time-resolved (3-h)

843 PM$_{2.5}$ samples in the rural site of NCP during the whole study period, Period 1 (P1) and Period 2

844 (P2).

Compounds	Whole period (N=117)			Period 1 (N=28)			Period 2 (N=13)		
	Range	Mean	SD	Range	Mean	SD	Range	Mean	SD
n-Alkanes	9.97~722.2	206.9	149.3	94.7~722.3	343.7	134.1	25.1~103.2	54.3	22.4
CPI (C$_{18}$-C$_{36}$)^a	1.08~8.62	2.47	1.12	1.38~4.67	2.85	0.87	1.08~3.5	1.64	0.59
Fatty acids	64.6~1777	514.4	384.3	206.7~1528	900.3	358.3	81.4~234.4	145.3	47.7
CPI (C$_{21:0}$-C$_{30:0}$)^b	2.26~9.15	4.24	1.14	3.49~6.11	4.21	0.64	2.26~8.57	3.50	1.64
Fatty alcohols	3.18~975.9	192.6	187.4	62.4~638.2	322.0	150.7	16.6~100.2	33.9	22.6
Sugar compounds	15.9~2228	432.8	428.9	151.9~1727	718.0	403.1	39.7~241.3	93.2	52.9
galactosan (G)	1.03~97.78	18.5	20.6	2.16~97.8	29.5	27.9	1.45~13.3	4.61	3.13
mannosan (M)	0.69~54.82	9.78	10.4	1.61~54.8	15.0	13.3	0.96~6.63	2.83	1.43
levoglucosan (L)	5.56~1447	240.1	287.8	29.3~1428	404.0	344.0	11.2~123	47.8	26.2
L/M ratio	4.03~71.8	22.8	8.85	13.9~71.8	29.7	12.2	11.3~23.1	18.0	4.28
L/(G+M) ratio	1.38~19.3	8.05	2.59	5.3~19.3	10.1	3.41	4.58~10.2	6.77	1.97
PAHs	1.11~48.5	12.0	11.0	4.21~37.7	18.6	11.0	1.25~5.01	2.33	0.98
Hopanes	0.66~10.81	3.46	2.38	0.86~9.97	4.40	2.48	1.14~2.28	1.81	0.31
Phthalate esters	17.7~219.9	84.9	41.3	68.8~183.1	111.5	32.7	31.5~100.8	51.1	18.1
Phthalic acids	17.1~487.2	154.5	93.9	91.3~388.6	211.0	87.1	17.1~81	46.3	17.1
Isoprene SOA tracers	11.1~404.1	111.9	85.8	48.3~404.1	208.5	104.9	34.8~127.5	57.0	29.4
Monoterpene SOA tracers	11.1~166.2	66.1	31.2	37.3~166.2	85.3	34.9	26.7~64.5	44.6	12.6
β-Caryophyllinic acid^c	0.49~77.7	17.4	17.1	4.6~77.8	34.7	20.8	2.44~6.28	4.08	1.21
DHOPA^d	1.59~35.3	9.36	7.15	4.06~35.3	15.6	9.80	2.7~6.99	4.16	1.42
Total measured organics	176.9~6249	1806	1308	843.3~5499	2973	1219	334.2~913.7	537.9	151.1
Total organics_C/OC^e (%)	3.19~16.0	6.99	1.97	3.43~8.86	6.43	1.36	3.77~8.61	6.41	1.27

845 ^{a} CPI (C$_{18}$-C$_{36}$): carbon preference index for *n*-alkanes, (C$_{19}$+C$_{21}$+C$_{23}$+C$_{25}$+C$_{27}$+C$_{29}$+C$_{31}$+C$_{33}$+C$_{35}$)/

846 (C$_{18}$+C$_{20}$+C$_{22}$+C$_{24}$+C$_{26}$+C$_{28}$+C$_{30}$+C$_{32}$+C$_{34}$).

847 ^{b} CPI (C$_{21:0}$-C$_{30:0}$): carbon preference index for fatty acids, (C$_{22:0}$+C$_{24:0}$+C$_{26:0}$+C$_{28:0}$+C$_{30:0}$)/ (C$_{21:0}$+C$_{23:0}$+C$_{25:0}$+C$_{27:0}$+C$_{29:0}$).

848 ^{c} β-Caryophyllinic acid: a tracer of β-caryophyllene-derived SOA.

849 ^{d} DHOPA: 2,3-dihydroxy-4-oxopentanoic acid, a tracer of toluene-derived SOA.

850 ^{e} All the quantified organic compounds were converted to their carbon contents to calculate the OC ratios.

Figure Captions

Figure 1. Backward trajectories of air masses (a,c) (provided by NOAA HYSPLIT modeling system, http://ready.arl.noaa.gov/HYSPLIT.php), and fire spots (b,d) (provided by Fire Information for Resource Management System, FIRMS, https://firms.modaps.eosdis.nasa.gov/firemap/), during Period 1 (P1) (Jun 13th 21:00-16th 15:00, 2013) and Period 2 (P2) (Jun 22nd 12:00-24th 06:00, 2013). Sampling site represented as purple star.

Figure 2. Temporal variations of $PM_{2.5}$, OC, EC, and WSOC during the whole sampling period. Shadows denote the two representative periods.

Figure 3. Linear correlations of OC with WSOC (a), levoglucosan with OC and WSOC(b).

Figure 4. Diurnal variation of OC/EC (a), WSOC/OC and levoglucosan/OC (b).

Figure 5. Temporal variations of ten organic compound classes detected in the summertime $PM_{2.5}$ samples at the rural site of NCP.

Figure 6. Temporal variations of organic tracers for biomass burning (a), and secondary products derived from α-/β-pinene (b-d), β-caryophyllene (e), and toluene (f).

Figure 7. Molecular distributions of n-alkanes (a and d), fatty acids (b and e), and fatty alcohols (c and f) in the $PM_{2.5}$ of the rural area.

Figure 8. Linear correlations of fatty acids (a), fatty alcohols (b), 3-hydroxyglutaric acid (c), and β-caryophyllinic acid (d) with levoglucosan.

Figure 9. Diurnal variation of the detected organic compound classes.

Figure 10. Diurnal variation of the SOA tracers derived from oxidation of α-/β-pinene (a-d), β-caryophyllene (e), and toluene (f).

Figure 11. A comparison of the average contributions of different sources-derived organics (converted to carbon content) to OC during P1 and P2.

Figure 12. Contributions (above) of primary organic carbon from biomass burning (OC_{bb}) and fungal spores (OC_{fp}), and secondary organic carbon from isoprene (SOC_i), α-/β-pinene (SOC_p), β-caryophyllene (SOC_p), and toluene (SOC_t) to OC in the time-resolved (3 h) rural aerosols, and their relative abundances (down). All the contributions were estimated by tracer-based method.

Figure 13. Average contributions of direct emissions from biomass burning (BB) and fungal spores (OC_{fp}), secondary oxidation from isoprene (SOC_i), α-/β-pinene (SOC_p),β-caryophyllene (SOC_p), and toluene (SOC_t) to OC in P1 and P2. All the contributions were estimated by tracer-based method.

887
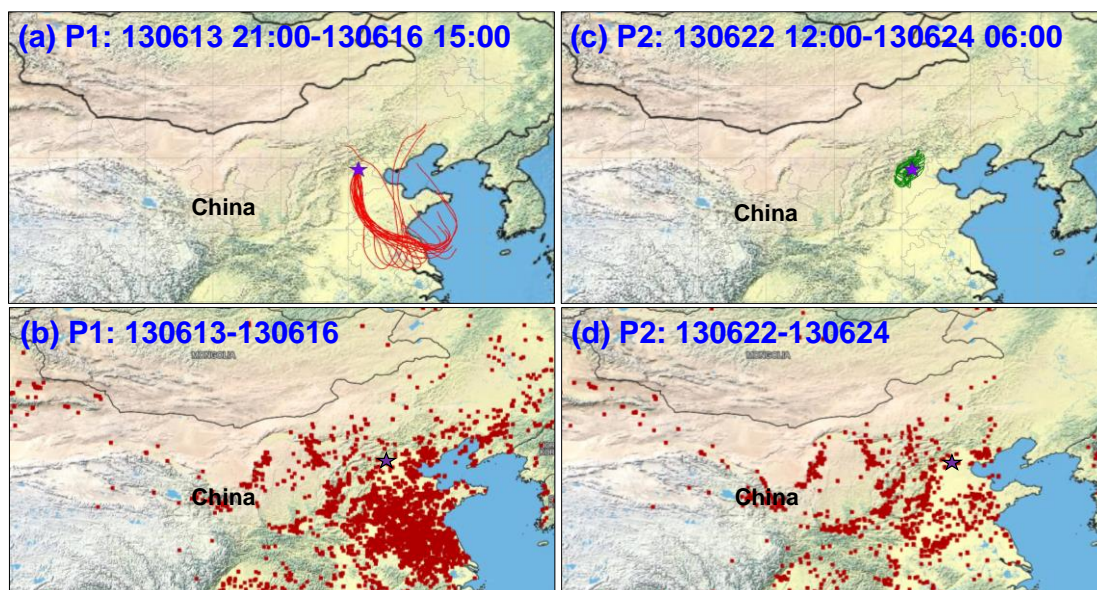
888

Figure 1. Backward trajectories of air masses (a,c) (provided by NOAA HYSPLIT modeling system, http://ready.arl.noaa.gov/HYSPLIT.php), and fire spots (b,d) (provided by Fire Information for Resource Management System, FIRMS, https://firms.modaps.eosdis.nasa.gov/firemap/), during Period 1 (P1) (Jun 13th 21:00-16th 15:00, 2013) and Period 2 (P2) (Jun 22nd 12:00-24th 06:00, 2013). Sampling site represented as purple star.

894
895
896
897
898
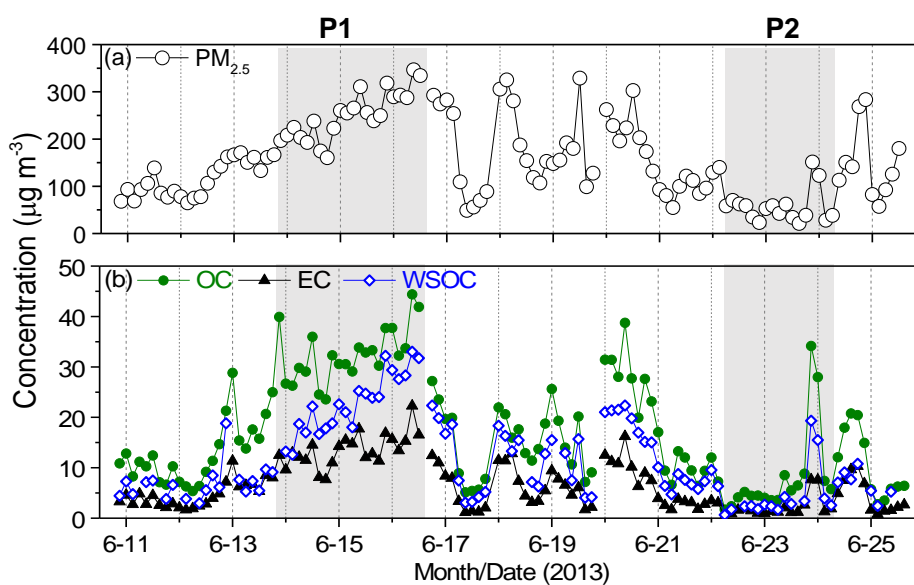
899

Figure 2. Temporal variations of $PM_{2.5}$, OC, EC, and WSOC during the whole sampling period. Shadows denote the two representative periods.

902

903
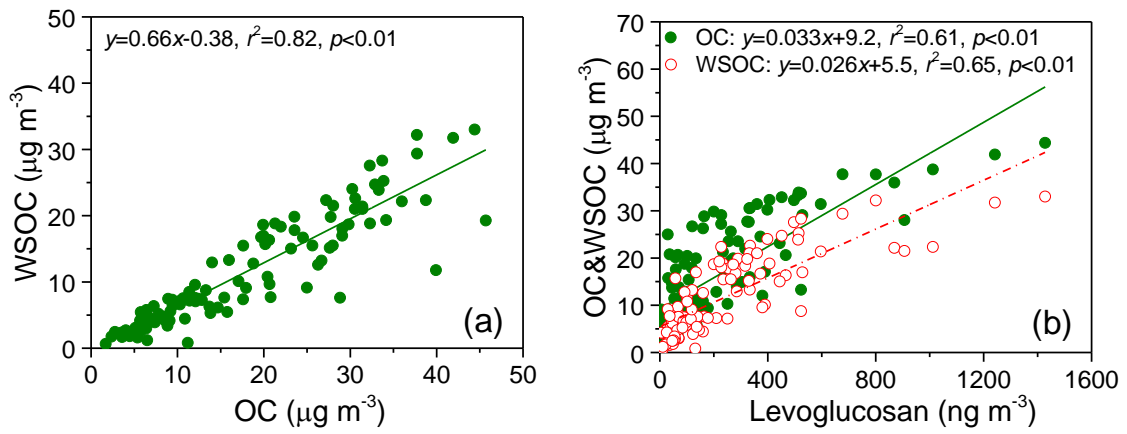
904

905   Figure 3. Linear correlations of OC with WSOC (a), levoglucosan with OC and WSOC(b).

906

907

908
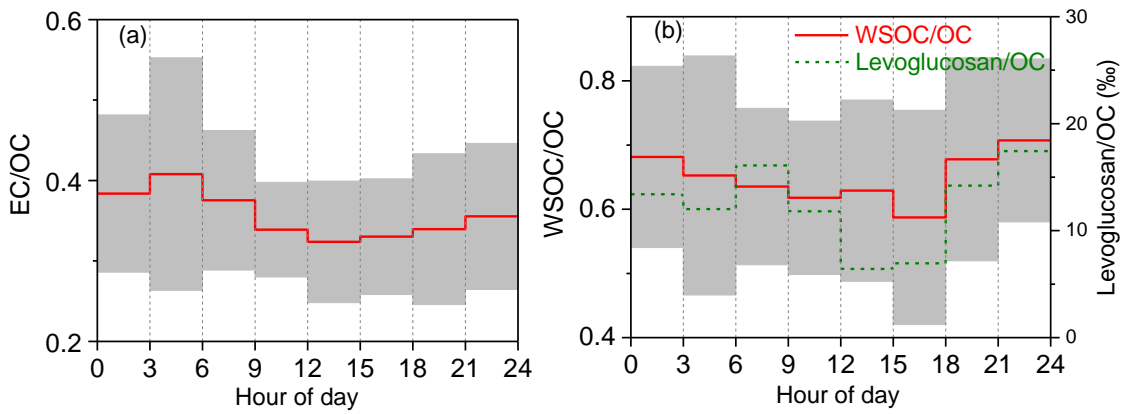
909

910   Figure 4. Diurnal variation of OC/EC (a), WSOC/OC and levoglucosan/OC (b).

911
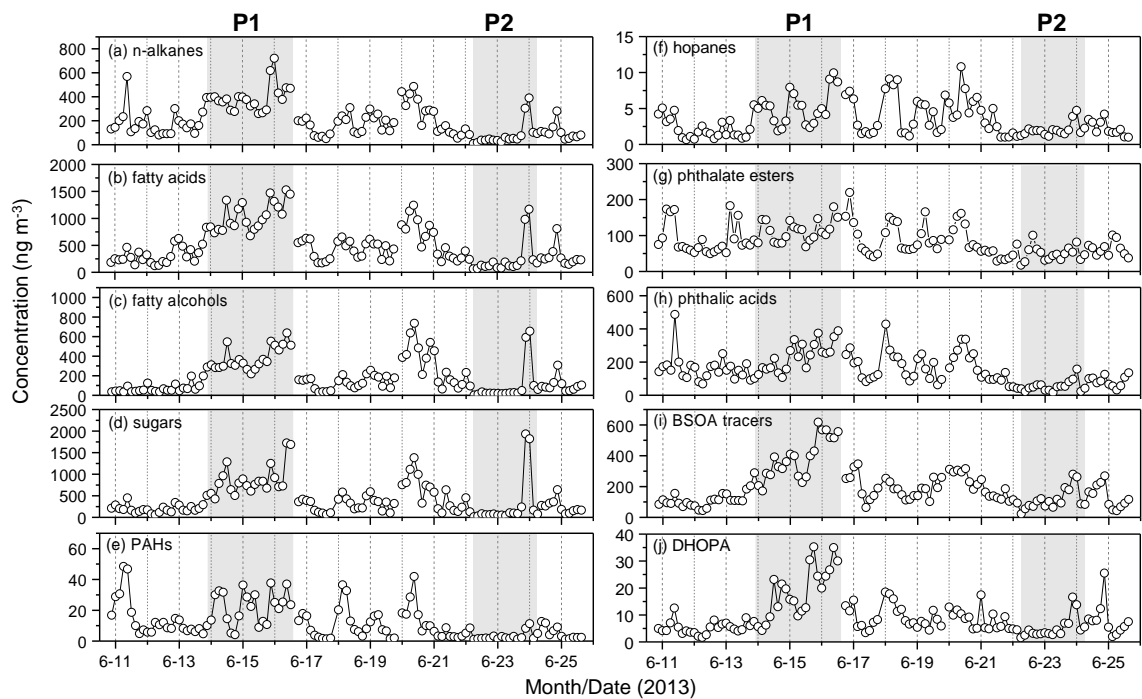
912

Figure 5. Temporal variations of ten organic compound classes detected in the summertime $PM_{2.5}$

samples at the rural site of NCP.

915

916
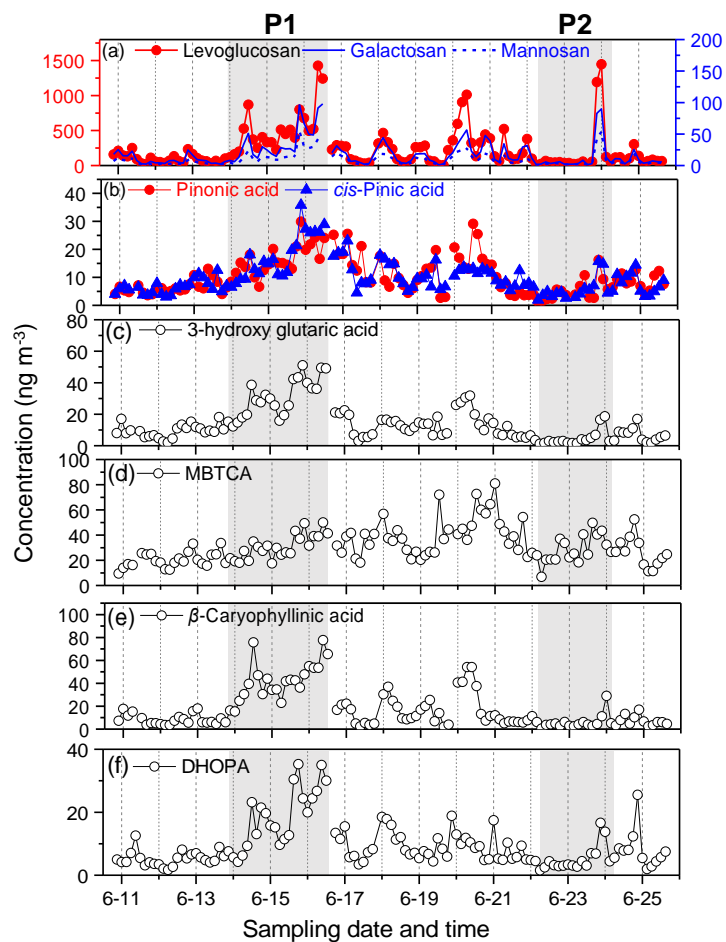
917

918 Figure 6. Temporal variations of organic tracers for biomass burning (a), and secondary products

919 derived from α-/β-pinene (b-d), β-caryophyllene (e), and toluene (f).

920
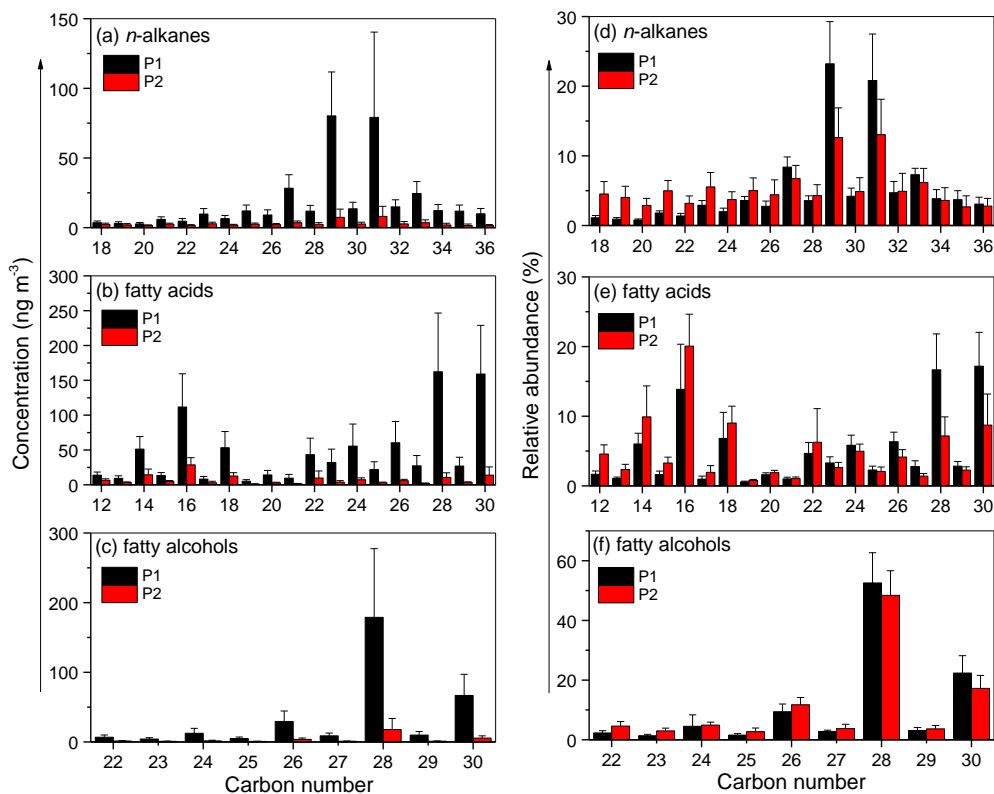
921

922 Figure 7. Molecular distributions of *n*-alkanes (a and d), fatty acids (b and e), and fatty alcohols (c and

923 f) in the PM$_{2.5}$ of the rural area.

924
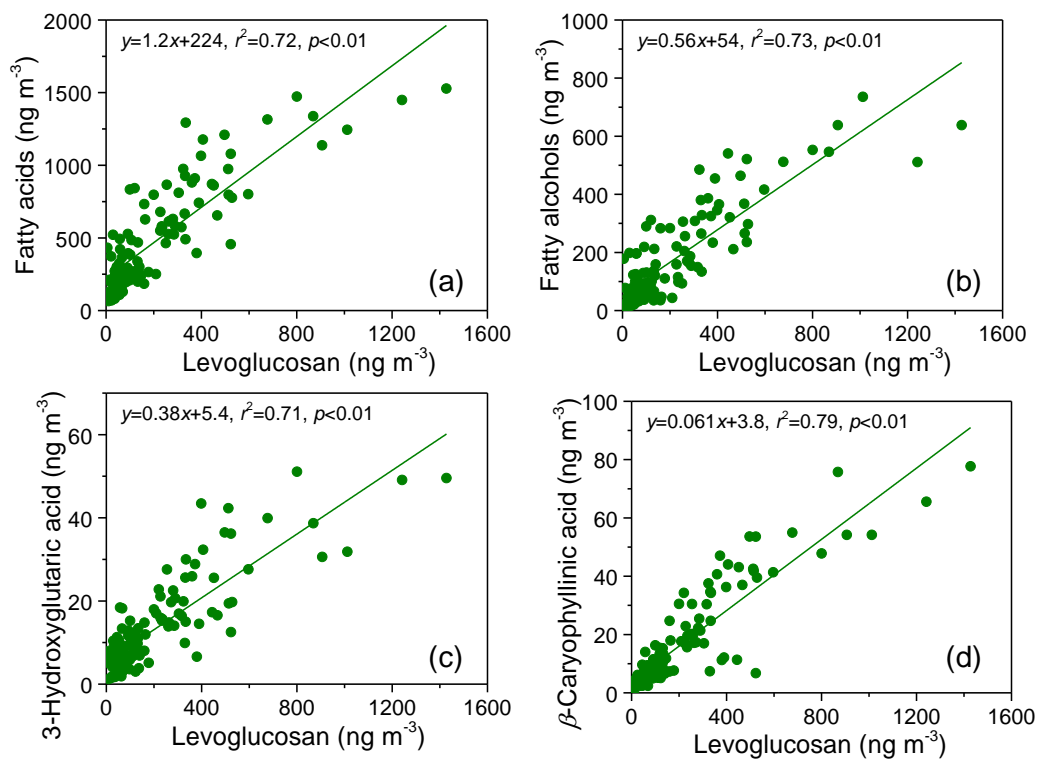
925

926 Figure 8. Linear correlations of fatty acids (a), fatty alcohols (b), 3-hydroxyglutaric acid (c), and β-

927 caryophyllinic acid (d) with levoglucosan.
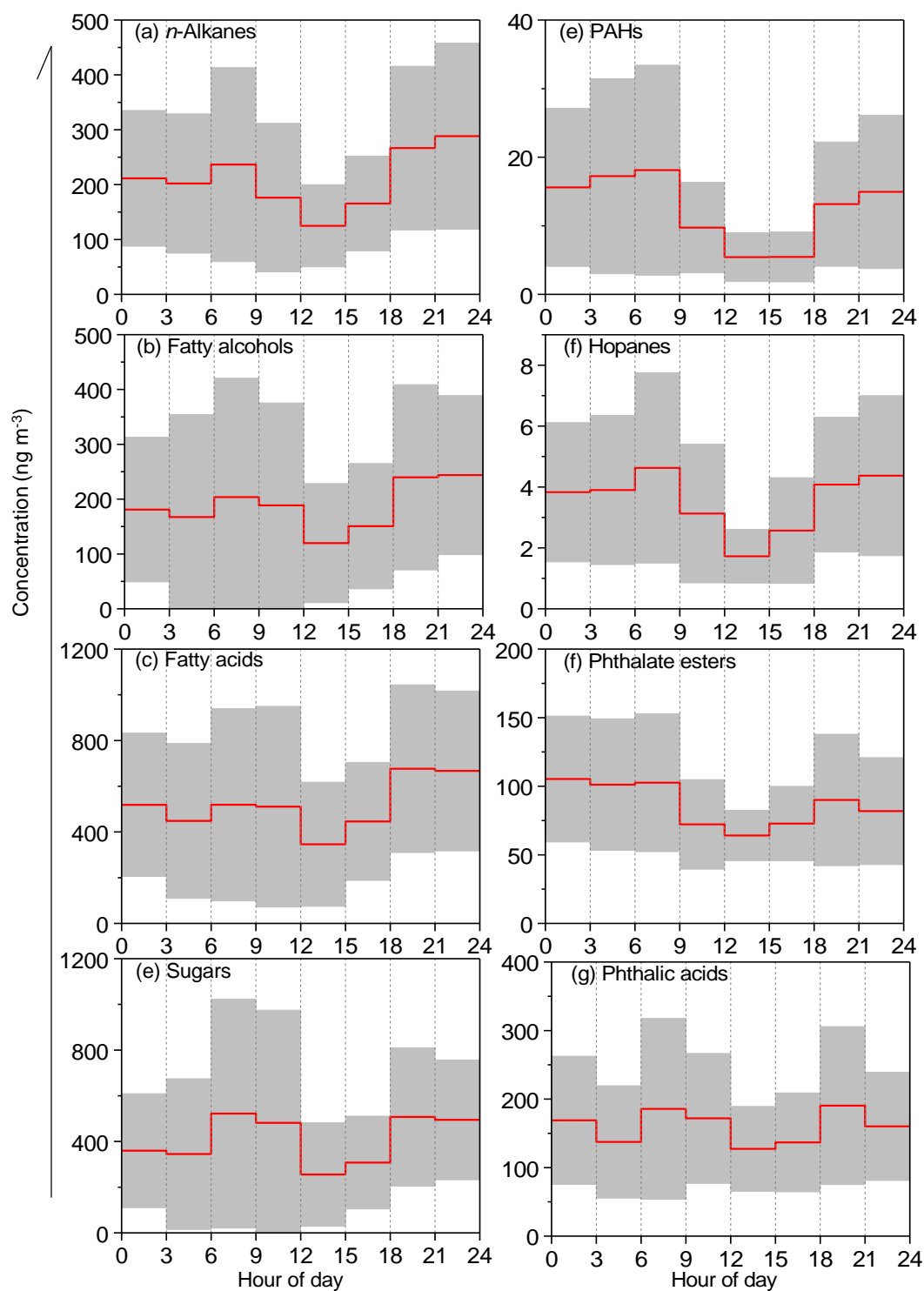
929

930 Figure 9. Diurnal variation of the detected organic compound classes.

931

932

933

934

935
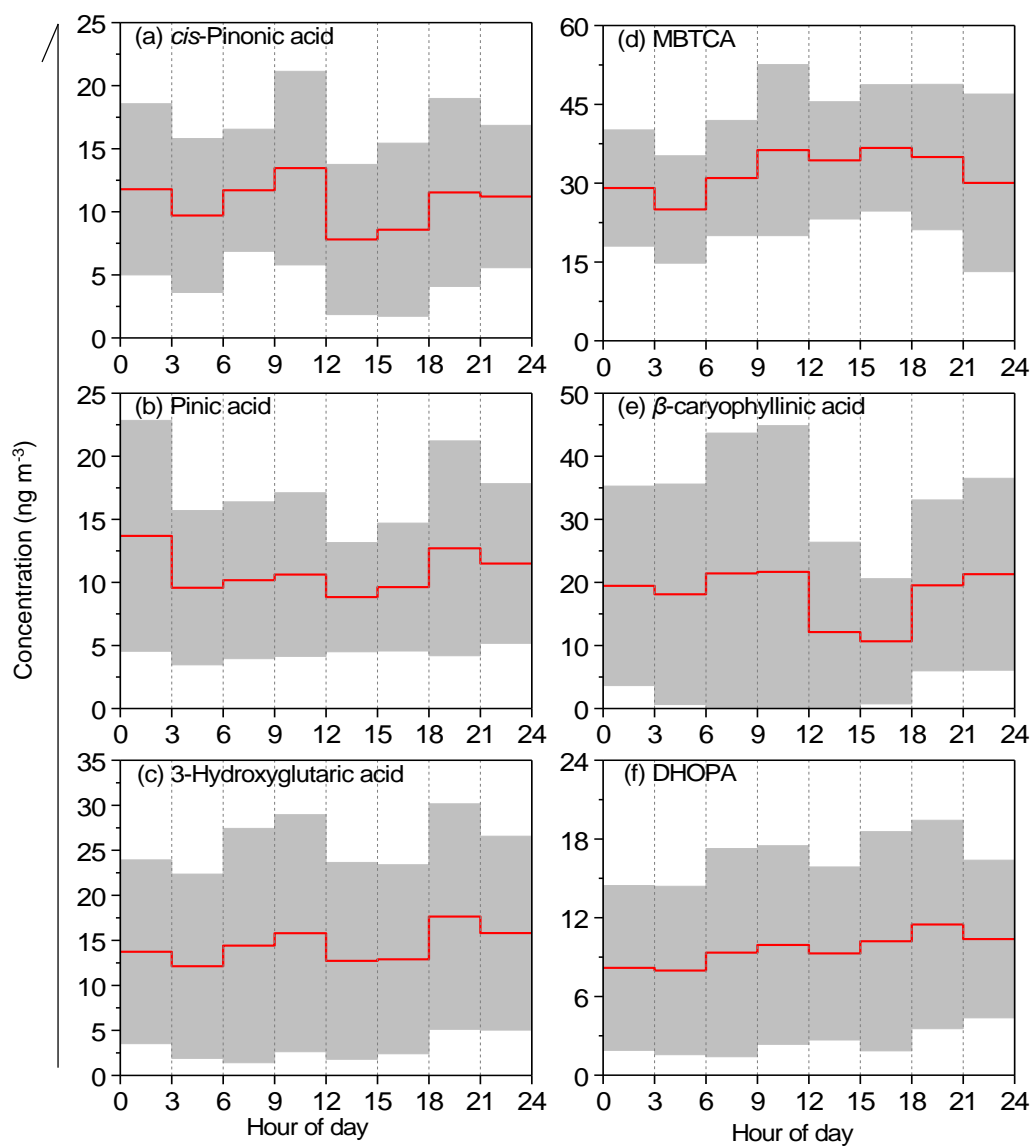
936

937 Figure 10. Diurnal variation of the SOA tracers derived from oxidation of *α-/β*-pinene (a-d), *β*-
938 caryophyllene (e), and toluene (f).

939

940
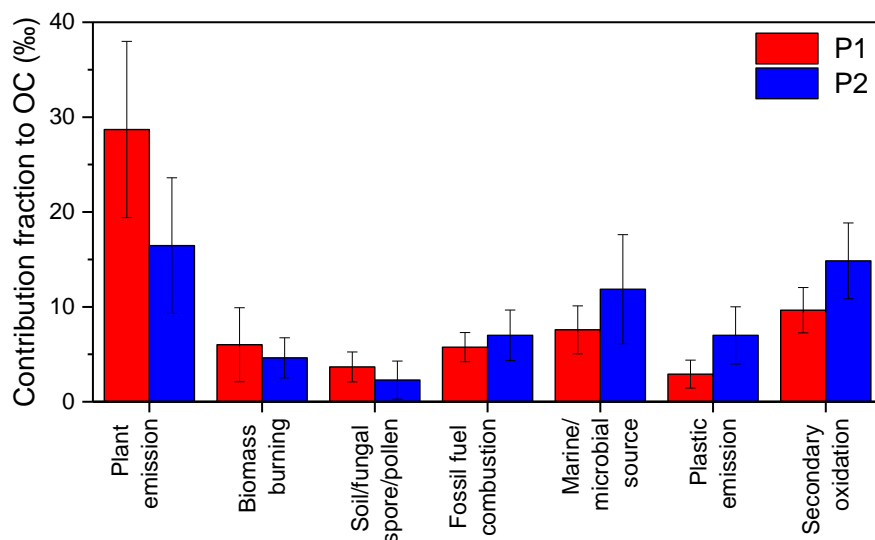
941
942 Figure 11 A comparison of the average contributions of different sources-derived organics (converted
943 to carbon content) to OC during P1 and P2.

944
945
946
947
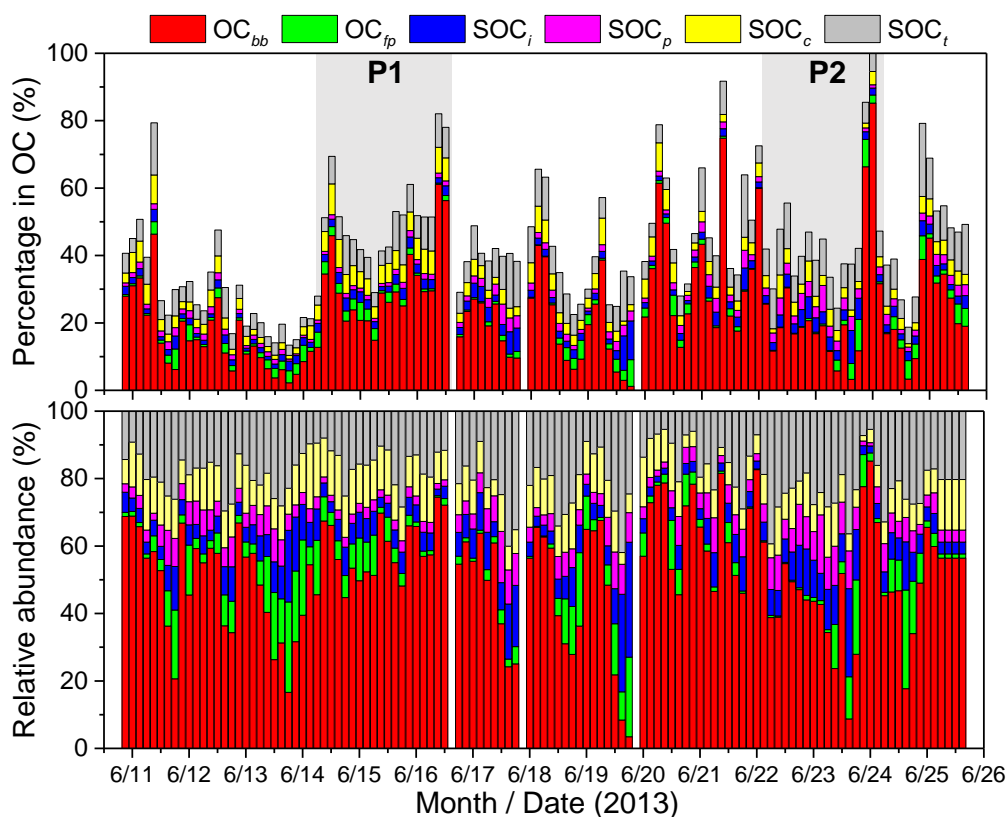
948
949 Figure 12. Contributions (above) of primary organic carbon from biomass burning (OC_{bb}) and fungal
950 spores (OC_{fp}), and secondary organic carbon from isoprene (SOC_i), α-/β-pinene (SOC_p), β-
951 caryophyllene (SOC_p), and toluene (SOC_t) to OC in the time-resolved (3 h) rural aerosols, and their
952 relative abundances (down). All the contributions were estimated by tracer-based method.
953

954

P1: OC=33 µg m⁻³ P2: OC=8.6 µg m⁻³

955

956 Figure 13. Average contributions of direct emissions from biomass burning (BB) and fungal spores

957 (OC$_{fp}$), secondary oxidation from isoprene (SOC$_i$), α-/β-pinene (SOC$_p$), β-caryophyllene (SOC$_p$), and

958 toluene (SOC$_t$) to OC in P1 and P2. All the contributions were estimated by tracer-based method.

959

960